

Reservoir zonation and discrimination using the routine core analyses data: the Upper Jurassic Sab'atayn sandstones as a case study, Sab'atayn basin, Yemen

Bassem S. Nabawy · Nabil A. S. A. Al-Azazi

Received: 30 January 2014 / Accepted: 15 September 2014 / Published online: 26 September 2014
© Saudi Society for Geosciences 2014

Abstract Sab'atayn basin is one of the two main hydrocarbon fields in Yemen. The present study is a trial to use the measured conventional core analysis data to define the potential reservoir zones in Alif and Seen members in Sab'atayn basin and to discriminate them into conductive and superconductive zones, and into potential and impervious zones using the concept of Reservoir Quality index (RQI), the Flow zone Index (FZI), and the Reservoir Potentiality Index (RPI). Samples from Alif and Seen members are composed mostly of pebbly quartz arenite, sometimes of dolomitic and ferruginous quartz arenite. Based on the petrophysical behavior, the studied Alif member is subdivided into three petrophysical facies in Alif 003 well and into two facies in Alif 005 well. Seen member is also subdivided into two petrophysical facies in Alif 005 well. The bulk density of the measured Alif and Seen samples is dependent mostly on the measured porosity with no dependence on the grain density. Due to the measuring technique, summation fluid porosity shows scattered data and is not recommended to be used for further development and exploration of future plans in the studied field. The reservoir zonation and discrimination shows a main reservoir body in Alif member in both Alif 003 and Alif 005 wells, with very good and excellent potentiality (RPI, 4–5) in Alif 003 well. The reservoir potentiality decreases to the southwest of the field in Alif 005 well, where the RPI varies from 2 to 4, ranked as fair to very good. Downward, Seen member is characterized mostly by negligible, poor to fair petrophysical data in the most top parts (RPI, 1–3). The quality controlled

parameters, RPI and FZI, are mostly controlled by horizontal permeability 'K' and can be calculated precisely in terms of it.

Keywords Reservoir zonation · Reservoir potentiality · Sab'atayn · Permeability · Porosity · Yemen

Introduction

Yemen is located in the south-west (SW) corner of the Arabian Peninsula, bordered by the Red Sea to the west, the Gulf of Aden to the south, and the Arabian Sea to the southeast (SE). It was driven by the Pangea breaking in the Mesozoic that formed the Gulf of Aden, Red Sea, and the Arabian Peninsula in the Cenozoic.

The geology and lithostratigraphy of Yemen were studied by many authors, e.g., Beydoun (1964), Powers et al. (1966), Beydoun and Greenwood (1968), Hughes and Clarke (1988), Haitham and Nani (1990), Paul (1990), Hughes and Beydoun (1992), Bott et al. (1992), Schlumberger (1992), Beydoun et al. (1993), etc.

Two major tectonic periods formed the tectonic evolution of Yemen. The first event took place in the Late Jurassic–Early Cretaceous, when three rift basins developed within Gondwana land: the Marib-Shabwa, the Sir-Sayun, and the Jeza-Qamar basins. The second major tectonic activity in the Cenozoic was related to the opening of the Gulf of Aden and the Red Sea and the collision of the Arabian Peninsula with Eurasia. At the end of the syn-rift phase, the Sab'atayn (Marib-Shabwa) basin became isolated from the sea, maintaining a periodically opened marine passage, which supplied saline water into the basin. The geographic separation and the warm climate gave rise to massive evaporation and deposition of major salt sequence called Sab'atayn Formation (Csato 2005).

Recently, many oil discoveries have been achieved in Yemen with estimated oil reserves reaching up to 9.718 billion

B. S. Nabawy (✉)
Department of Geophysical Sciences, National Research Centre,
Cairo, Egypt
e-mail: bsnabawy@yahoo.co.uk

N. A. S. A. Al-Azazi
Faculty of Oil and Minerals, Aden University, Aden, Yemen

barrels. There are many promising areas located at 12 sedimentary basins.

Yemeni petroleum production is mostly coming from two rift basins: the Sab'atayn basin (Marib-Shabwa basin) in the western Yemen and the Masila-Jeza basin in eastern Yemen. These eastern and western basins are largely separated by a structural high known as the Mukalla or Jahi-Mukalla High. The Sab'atayn basin is the most important promising and productive basin in Yemen. It is located in Marib, Shabwa, and part of Al-Jawf Governorates. Sab'atayn basin (Marib–Shabwa–Hajr Basin) was studied by Beydoun et al. (1998) and studied as Marib-Shabwa basin by Brannin et al. (1999) and Csato et al. (2001).

Due to the increasing the hydrocarbon exploration activity extensively after 1990, the basin evolution in Yemen has been revised by Redfern and Jones (1995), Ellis et al. (1996), and Beydoun et al. (1996). The gross tectono-stratigraphic development of Sab'atayn basin has recently been subdivided by Redfern and Jones (1995) into several linked grabens and half grabens.

The petroleum-bearing grabens of Yemen are interpreted to be the result of a failed arm of a triple junction that occurred in Late Jurassic time (Kimmeridgian) (Greenwood et al. 1980; Husseini 1989; Jungwirth and As-Saruri 1990; Schlumberger 1992; Redfern and Jones 1995, Csato et al. 2001).

Although the petroleum-bearing grabens are considered to be of Late Jurassic age, their origins can be traced back to Precambrian fault systems. During Precambrian time, the area underwent a major collision and terrain accretion from about 955 to 615 Ma ago (Husseini 1989; Whitehouse et al. 1998; Ahlbrandt Th. S 2002).

Yemen concessions can be classified into 105 concession blocks; 13 of these blocks are oil-producing. Five blocks out of the producing blocks are located in Sab'atayn basin (Block 18, Jannah 5, Damis S1, West Ayad 4, and Al-Uuqlah S2).

In 1984, the Yemen Hunt Oil Company (YHOC) announced the first commercial discovery in Yemen in Alif Oil Field in block 18. The Alif Oil Field (block 18), the target of the present study, is located in the middle of Sab'atayn basin between latitudes 14° 40' and 16° 30' N and longitudes 44° 40' and 48° 30' E, it has a northwest (NW)–SE general direction (Fig. 1). It is a giant hydrocarbon field based on subsequent delineation development drilling with estimated recoverable reserves of approximately 500 million bbl of oil and 4 trillion standard cubic feet of gas.

The main aim of the present study is to study the storage capacity properties and to rank the reservoir quality of Alif and Seen members in Alif Oil Field in Sab'atayn basin. Using the oil and water saturation data in integration with the storage capacity data enables reservoir zonation and discrimination of super conductive zones in the studied oil field. The reservoir quality and flow zone discrimination were applied using the technique published by Amafeule et al. (1993) which allows a more precise reservoir discrimination using the permeability and porosity data.

The reservoir quality index (RQI) can be used to qualify the flow character of a reservoir and provide a good relationship between petrophysical properties at the core plug scale and the well bore scale. It helps for a more qualified reservoir slicing. It was successfully applied by many authors to determine the reservoir quality, e.g., Tiab and Donaldson 1996; Al-Dhafeeri and Nasr-El-Din 2007; Othman et al. 2008.

Geologic setting

Sab'atayn basin includes two main basins, the Marib-Shabwa and the Balhaf basins. It propagates southeastwards from the Marib sector to the Shabwa and then to the Hajr sector. Balhaf basin is separated from the Sab'atayn basin by the narrow Al Aswad massif.

The Amran group in Sab'atayn basin is widely exposed in the northern, western, and southern parts of Yemen, and due to its hydrocarbon potentiality, it has been an interesting research topic to many authors (e.g., Beydoun (1964), Geukens (1966), Abou Khadrah (1982), Abou Khadrah et al. (1983), El-Anbaawy (1984), Diggenees et al. (1988), El-Anbaawy and Al-Thour (1989), Al-Thour (1997, 2000), El-Nakhal (1990), Al-Wosabi (2003, 2005), As-Saruri et al. (2010), etc.

El-Anbaawy (1984) discussed the sedimentological evolution of the Upper Jurassic Amran series in northern Yemen. He subdivided it into four formations: Shuqra, Sab'atayn/Madbi, Jabal Salab, and Wadi Al-Hajr Formations. Beydoun (1964) and Beydoun et al. (1998) subdivided Amran group 'series' in southern Yemen, from the older to the recent, into four formations, namely Nayfa, Sab'atayn, Madbi, and Shuqra formations (Fig. 2). Following Beydoun et al. (1998), the Upper Jurassic sequence in Alif field is subdivided into the following formations.

Nayfa formation, Upper Tithonian to Berriasian

It is composed mainly of limestone sequences. Its type section was assigned by Beydoun (1964) as porcellaneous limestone sequence intercalated with dolostones and shale bands at Al-Ma'abir in Wadi Hajr in Hadramawt province. It was encountered in all the main Yemeni rifted basins, and it was deposited mainly in open marine environments (Beydoun et al. 1998).

In the subsurface of the Marib sector of the Marib-Shabwa basin, the Nayfa informally referred to as the Azal Formation by YHOC (Schlumberger 1992).

Sab'atayn formation, Lower to Upper Tithonian

The Sab'atayn Formation, the target of the present study, is the main oil-bearing formation in Alif oil field represents the middle part of the Amran Group (Dogger-Malm age following Beydoun et al. 1998).

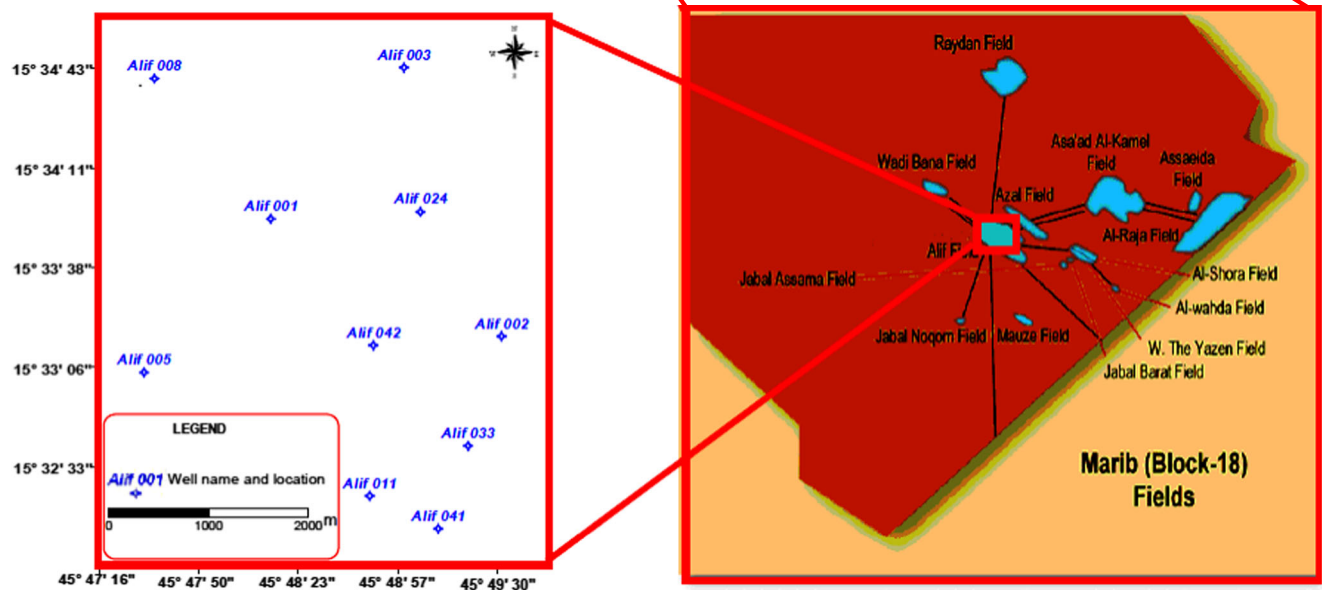
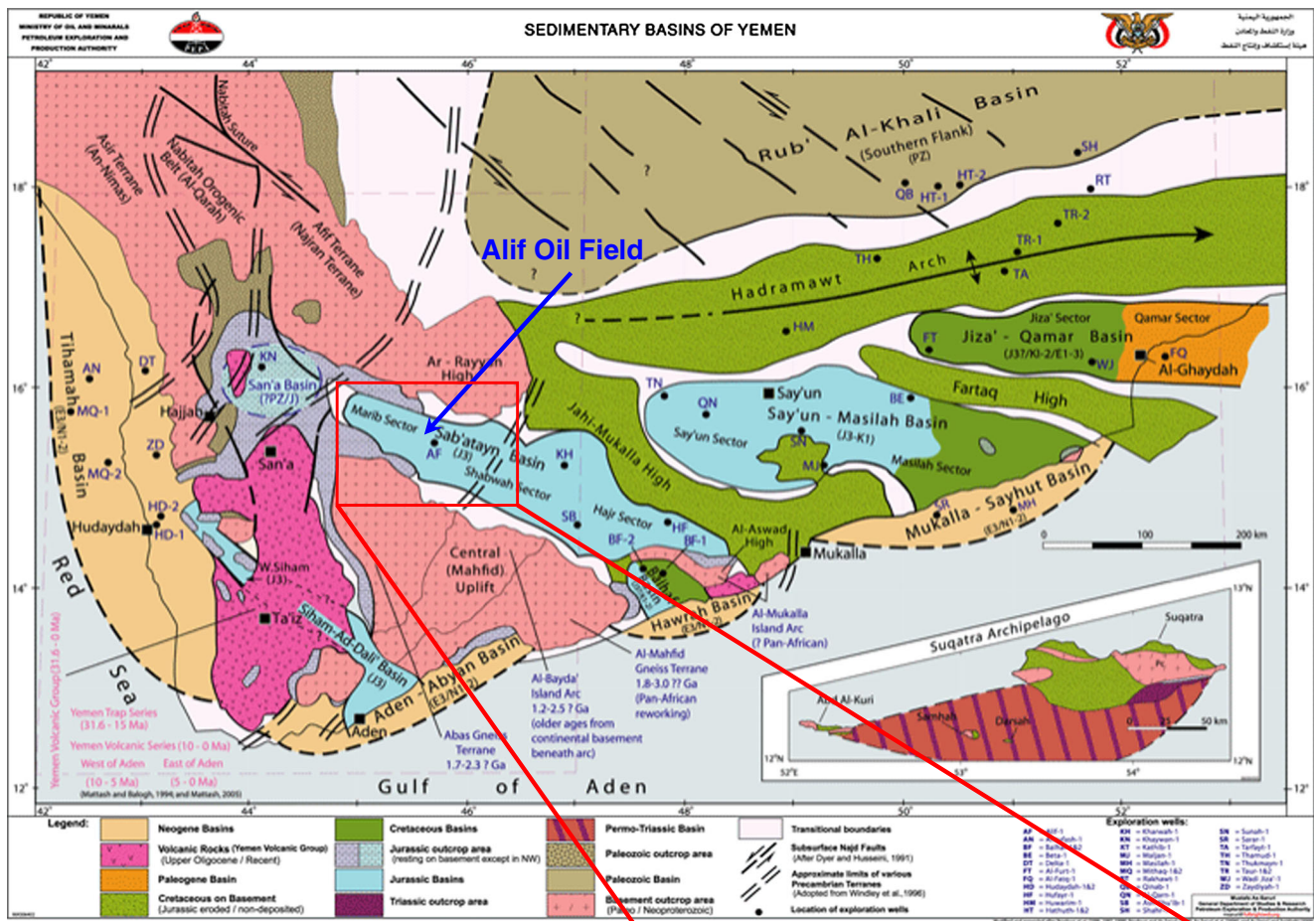


Fig 1 Location map showing the study area and the oil promising sedimentary basins of Yemen (Beydoun et al. 1998)

In the study area, Sab'atayn Formation is subdivided into Safir member (Upper Tithonian), Alif member (Middle Tithonian to

Upper Tithonian), Seen member (Lower Tithonian to Middle Tithonian), and Yah member (Lower Tithonian).

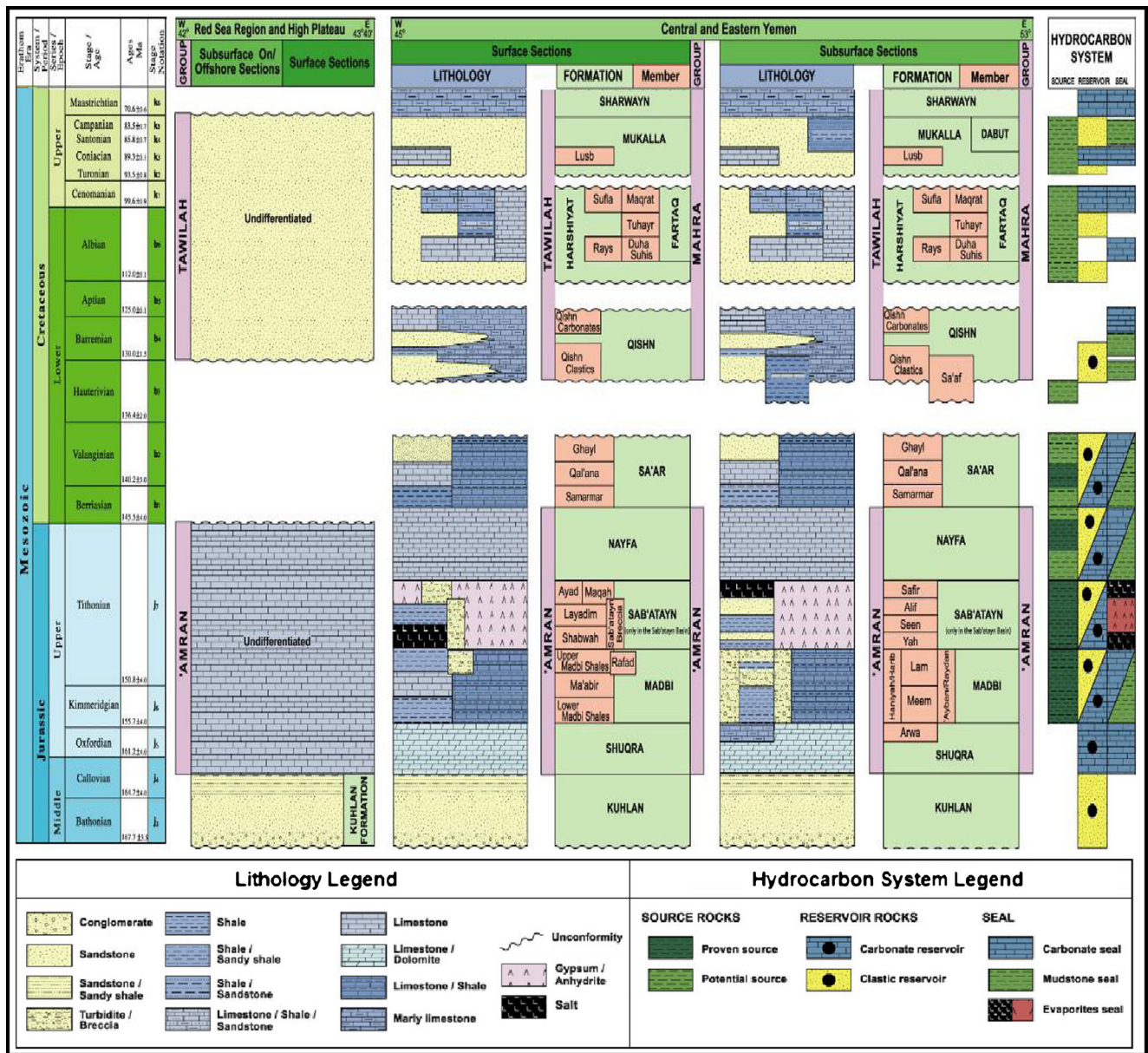


Fig 2 Mesozoic lithostratigraphic column and hydrocarbon systems in Yemen

The main producing reservoirs in the Marib-Jawf sector occur within the Alif and Seen Members of the Upper Jurassic Sab'atayn Formation and that the hydrocarbon traps were formed as low angle fault blocks and sealed by the main salt unit belongs to Safir Member. Madbi shale is the main source rock for hydrocarbons in this sequence.

The maximum thickness of Sab'atayn Formation is about 2,771 ft in Alif003 well while the minimum thickness reaches the values of 2,200 ft in Alif 005 well.

Safir member

It is composed of a thick halite with subordinate anhydrite intercalated with shales and sandstones with minor

argillaceous dolomitic limestone in five consequent cycles. It acts as an excellent seal rock for the underling Alif Member reservoir. It sometimes contains thin local reservoirs.

Alif member

Alif member conformably overlies the Seen member and unconformably overlain by the Safir member. It consists of sandstones with subordinate interbeds of shales, anhydrite lenses, and dolomitic limestones (Beydoun et al. 1998). The Alif member is considered as the main reservoir in the Marib-Shabwa basin and comprises over 90 % of recoverable oil. It attains its maximum thickness in Alif 003 well (708 ft).

Seen member

Seen member is conformably underlain by the Yah member and overlain by the Alif member. It consists mostly of sandstones intercalated with shales. Sandstones predominate in the upper parts while the shales predominate in the lower sequences. The upper parts contain some thin bands of anhydrite (Beydoun et al. 1998).

Locally, Seen member pinches out to the NE side of the Shabwa sector. It is not encountered in Alif 003 well (Fig. 3).

Yah member

Yah member disconformably overlies the Madbi Formation at its type section. It consists mainly of sandstone intercalated

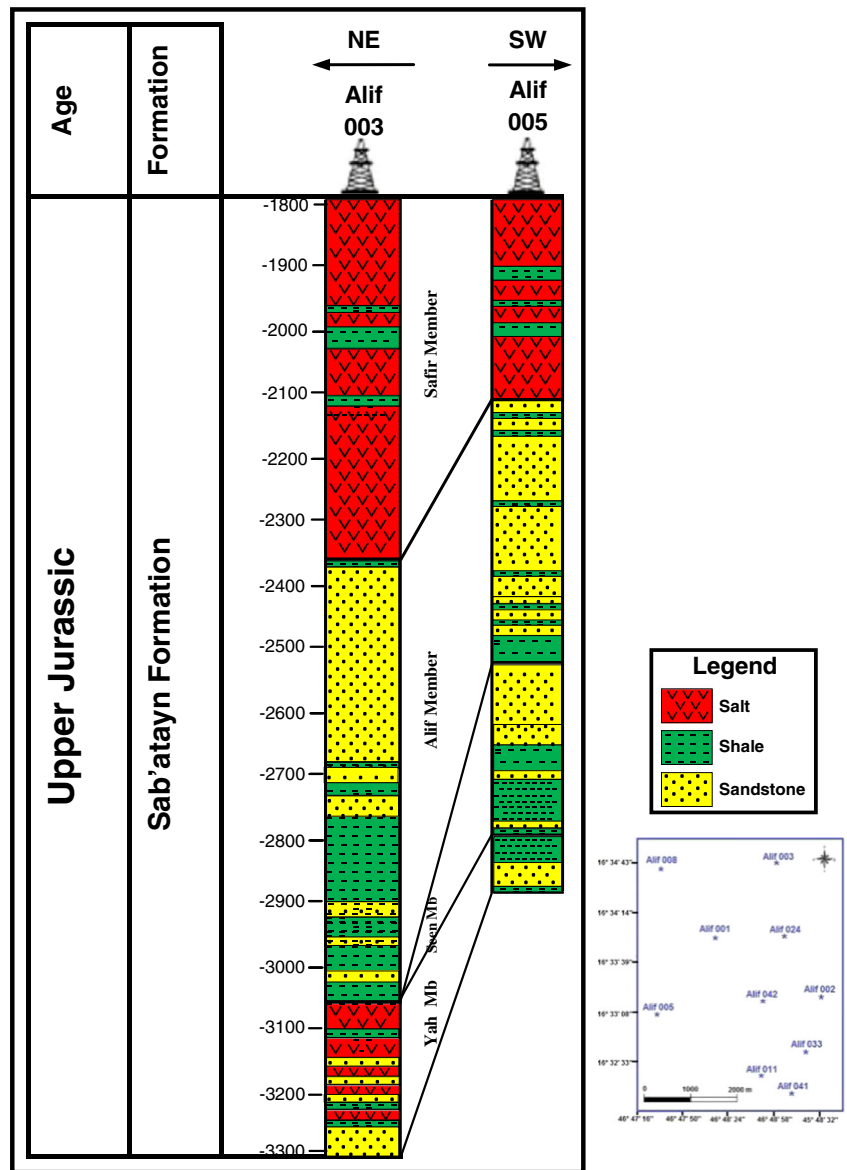
with mudstones, and locally with limestone and halite. Its maximum thickness is encountered in Alif 003 well (252 feet). It pinches out to the SE towards the end of the Shabwa sector (Beydoun et al. 1998).

Madbi formation, Lower Kimmeridgian to Lower Tithonian

It consists of marl sequences, shaly, or gypsiferous, sometimes bituminous with abundant macro-fauna. It is rich in organic matter and considered as the main source rock for the hydrocarbon bearing rocks in Sab'atayn and Say'un-Masila basins (Beydoun et al. 1998). The marl sequences are intercalated with thin bands of marly, sandy, or fossiliferous limestones.

The Madbi Formation is subdivided into Harib Member (Lower Tithonian), Lam Member (Lower Tithonian), Meem

Fig 3 Lithostratigraphic correlation between the studied Alif and Seen members in wells Alif 003 and Alif 005, Sab'atayn Formation, Sab'atayn Formation, Yemen



Member (Kimmeridgian to Lower Tithonian), Raydan Member (Kimmeridgian to Lower Tithonian), Haniyah Member (Kimmeridgian to Lower Tithonian), and Ayban Member (Kimmeridgian to Lower Tithonian).

Shuqra formation (Oxfordian to Kimmeridgian)

It conformably underlies the Madbi Formation and conformably overlies the underlying Kuhlan Formation with a gradational contact. It consists predominantly of platform carbonates as lime mudstones, wackstones, and grainstones (Beydoun et al. 1998).

Basin evolution and structural outlines

During the Mesozoic, two main phases of rifting was effective in Yemen. The first was in the Kimmeridgian–Berriasian age, and the other was in the Hauterivian–Barremian (Redfern and Jones 1995; Ellis et al. 1996; Sharland et al. 2001).

The first phase began in the early Kimmeridgian in western Yemen causing accumulation of thick syn-rift deposits including the thick carbonates and shales of Madbi Formation (Beydoun et al. 1998; As-Saruri et al. 2010). The organic-rich intervals of Madbi Formation are the main source rocks for the Sab'atayn hydrocarbon-producing basin (Alaug et al. 2008, 2011; Hakimi et al. 2011a, b).

Thick carbonates and clastics were deposited during the second Hauterivian–Barremian rifting phase including the Sa'ar and Qishn formations.

In the latest Early Cretaceous, paralic clastics were deposited in western Yemen, while late syn-rift carbonates were deposited in eastern Yemen (Fartaq Formation of the Mahra Group). The transition between clastics and carbonates oscillated from west to east in the eastern part of Yemen as a result of sea-level changes, locally modified by remnant rift topography (Bott et al. 1992; Redfern and Jones 1995; Bosence 1997; Brannan et al. 1997).

Sab'atayn basin is NW–SE rift, following the Najd trend of the Precambrian basement of the Arabian Peninsula (Beydoun 1991, 1997, Bosence 1997). The Sab'atayn Basin is an asymmetric half-graben with a large central intra-basin high (Redfern and Jones 1995) that was active and controlled shallow marine sedimentation during the late Jurassic and Cretaceous.

This is flanked to the north by a NW-dipping and thickening half-graben (Northern Shabwa Depression, Ellis et al. (1996); or Sab'atayn and Hawag-Hajr troughs of Redfern and Jones (1995)) and a southwesterly dipping and thickening half-graben to the south Southern Shabwa Depression (Ellis et al. 1996) or Ataq Trough of Redfern and Jones (1995).

Electrical imaging logs (FMS-FMI) indicate southeasterly palaeo-currents within channel-fill sands (Gendrot 1995). The sands occur as lowstand deposits within depositional sequences

capped and sealed by high stand salts of the Sean and Safer Formations (Mitchell and Galbiati 1995; Mitchell and Kohles 1995) or Sab'atayn Formation (Beydoun 1997) generated during evaporative drawdown in the isolated Sab'atayn basin.

During the Late Jurassic, gentle eastward tilting and extension resulted in low-angle listric faults along a salt detachment (Seaborne 1995, 1996) which provide the trapping mechanism with the salt seal within the Alif fields (Mitchell and Galbiati 1995).

The structure contour map for the top of Alif Member indicates that the dominant structure in Alif field is a double-plunging anticline and that the area is affected by several parallel faults that have the trended NE–SW (Al-Azazi 2010).

Measured data

A complete set of conventional core analyses of 450 plug samples has been conducted for the order of Yemen Safer Exploration and production operation Company (SEPOC). The analyses include measuring bulk and grain density, summation fluids and helium porosity, nitrogen permeability, as well as water and oil saturation. Coring process was limited to two representative bore holes in Alif oil Field, in block no. 18, namely Alif 003 and Alif 005 wells (Fig. 1). The studied plugs are representative for the prospective zones in both wells, 262 plug samples for Alif-3 well, and 188 plug samples in Alif 005 well (Table 1).

Most of the studied samples of the Alif and Seen members are coarse-grained quartz arenite. Alif member is also presented by dolomitic and ferruginous quartz arenite samples, particularly in Alif 003 well.

The determined bulk density values of were found to vary from 1.81 to 2.40 g/cm³ for Alif Member in Alif 003 well and from 2.01 to 2.47 g/cm³ in Alif 005 well, whereas the bulk density for Seen Member in Alif 005 well varies from 2.07 to 2.56 g/cm³. The relatively low values (2.56 g/cm³) for the grain density of core-2 plugs, Alif 003 well, may be due to the presence of some light clay minerals. Helium porosity for samples from Alif 003 well varies from 11.5 to 31.9 % (ranked as fair to excellent; Nabawy et al. 2009), whereas it varies from 6.80 to 23.9 % (ranked as poor to very good) for Alif member in Alif 005 well. Seen member has poor to very good helium porosity (6.70 to 21.7 %), and permeability varies from 0.51 to 538.0 millidarcy (md) (ranked as fair to very good; Nabawy et al. 2009). Permeability of Alif member in both Alif 003 and Alif 005 wells varies from 1.6 to 13,500 and from 0.23 to 3824.0 md, respectively (Table 1). The oil saturation in Alif 003 well may reach up to 35.1 % with water saturation reaches up to 54.6 % in the upper parts of the member, whereas the water saturation increases greatly in the lower parts of the member reaching up to 95.1 % Sw. The same situation has been encountered in Alif 005 well,

Table 1 Number of studied samples (*N*), bulk and grain density (σ_b, σ_g), helium and fluid summation porosity (ϕ_{He}, ϕ_f), permeability (*K*), water saturation (*Sw*), oil saturation (*So*), Reservoir Quality Index (RQI), and Flow Zone Index (FZI) data for the studied plug samples, Sab'atayn Formation, Alif Oil Field, Yemen

Member	Depth (ft)	<i>N</i>		σ_b g/cm ³	σ_g g/cm ³	ϕ_{He} %	ϕ_f %	<i>K</i> md	<i>Sw</i> (%)	<i>So</i> (%)	RQI 0.00	FZI
Alif 003 well												
Alif member	Core-1 5,668.5–5,902.5	217 Plugs	Mean	2.08	2.66	21.8	22.0	4,675	31.5	7.48	4.34	15.5
			Min.	1.81	2.56	11.5	2.00	205.0	12.4	0.00	0.93	3.00
			Max.	2.40	2.72	31.9	32.6	13,500	54.6	35.1	7.74	27.5
	Core-2 5,965.5–5,989.5	45 Plugs	Mean	2.20	2.68	17.2	15.1	200.2	79.5	1.20	0.87	4.17
			Min.	2.11	2.63	11.7	10.3	1.6	65.7	0.00	0.09	0.42
			Max.	2.38	2.70	21.3	18.3	675	95.1	6.20	2.01	10.3
Alif 005 Well												
Alif member	Core-1 5,379.5–5,405.5	27 Plugs	Mean	2.10	2.65	20.8	22.5	811.1	33.5	0.10	1.8	7.1
			Min.	2.01	2.63	11.8	16.3	11.00	26.2	0.00	0.24	1.11
			Max.	2.39	2.71	23.9	32.1	3824.0	54.3	1.30	4.3	16.3
	Core-2 5600.5–5659.5	56 Plugs	Mean	2.18	2.65	17.6	17.4	135.5	42.2	0.9	0.7	3.0
			Min.	2.06	2.61	6.80	1.20	0.23	20.3	0.00	0.05	0.28
			Max.	2.47	2.68	22.3	24.7	810.0	94.0	8.3	2.1	9.1
Seen member	Core-3 5,778.5–5,874.5	105 Plugs	Mean	2.18	2.65	17.8	17.0	168.3	51.3	4.5	0.8	3.7
			Min.	2.07	2.60	6.70	1.10	0.51	19.10	0.00	0.06	0.36
			Max.	2.56	2.74	21.7	21.4	538.0	93.0	15.7	1.7	7.5

where the water saturation increases in the lower parts of both Alif and Seen members, *Sw* up to 94 %, which indicates approaching the Free Water Level at which *Sw* reaches to 100 %. Values of other saturation and storage capacity parameters are presented in details in Table 1.

For reservoir quality discrimination, the RQI, Normalized Porosity Index (NPI), and Flow Zone index (FZI) of Amaefule et al. (1993) were calculated as follows. The calculated data are shown in Table 1 for each coring range.

$$RQI = 0.0314 \sqrt{\frac{k}{\phi}}$$

Where *k* is permeability, in millidarcy, and ϕ is porosity, in volume fraction.

NPI is expressed as:

$$NPI = \frac{\phi}{1 - \phi}$$

RQI and NPI are then used to determine the FZI, which is used to qualify the flow character of the reservoir. FZI is expressed as follows:

$$FZI = \frac{RQI}{NPI} = \frac{0.0314\sqrt{k/\phi}}{\phi/(1 - \phi)}$$

The FZI is based on normalized porosity NPI, as well as the RQI whereas the RQI is based mostly on the permeability values.

In the present study, we tend to use another concept called Reservoir Potentiality Index (RPI) to discriminate and specify the rank of the reservoir potentiality based on the RQI and the FZI and taken the hydrocarbon and water saturation into consideration. RPI is taken as the arithmetic mean of the RQI and the FZI.

$$RPI = \frac{RQI + FZI}{2}$$

The reservoir zonation and discrimination has been done by accumulating depths having same reservoir rank together as main flow zones.

Petrography and diagenesis

To decipher the petrophysical behavior and the reservoir characterization of the studied Alif and Seen members, mineralogical composition and governing diagenetic factors must be taken into consideration.

Alif member is mostly made up of moderately to well sorted, fine- to coarse-grained quartz arenite. Petrographically, it can be distinguished into three microfacies: (1) quartz arenite; (2) dolomitic quartz arenite; and (3) ferruginous quartz arenite. Using SEM and XRD techniques indicate the presence of some authigenic dispersed clay minerals, mostly kaolinite, sometimes illite and montmorillonite. The quartz grains are mostly cemented together by silica cement as quartz arenite, by

carbonate cement as dolomitic quartz arenite and by iron oxides (hematite) and sulfides (pyrite) as ferruginous quartz arenite. On the other hand, Seen member is composed mostly of quartz arenite. The quartz grains are moderately to well sorted, fine- to coarse-grained, cemented together by silica cement (Al-Azazi 2010).

The diagenetic factors governing sedimentary rocks after deposition and accumulation have a great reducing or enhancing effect on their potentiality as hydrocarbon reservoirs. Dissolution and leaching out as well as fracturing are the most important porosity-enhancing processes. Cementation, compaction, pressure solution, authigenic clay minerals, and aggrading neomorphism, on the other hand, are the most important porosity-reducing diagenetic processes (Nabawy 2013).

Dissolution and leaching out is the dominant porosity-enhancing factor for both Alif and Seen members. It was strong enough to introduce both members as good reservoirs with good to very good porosity (15–25 %); sometimes porosity is excellent ($\varnothing > 25$ %). On the other hand, cementation and replacement is the main porosity-reducing factors. Silica cement as a quartz overgrowth is the main cement/matrix of Alif and Seen members. Carbonates (calcite and dolomite), ferruginous clays, and evaporates are other types of cement recorded for the studied sandstones. Silica cement may be a good indication for a long period of quartz and feldspar dissolution by low silica-invading solutions and pressure solution. Pressure solution is indicated by fractured, point, and sutured contact quartz grains in Alif Member (Al-Azazi 2010). Following Dutton and Land (1988), compaction of the intercalated argillaceous bands and the dissolution of biogenic silica in Alif and Seen members are thought to be another external source of silica.

Calcite cement is mostly presented by poikilotopic and drusy sparite. The quartz grains are occasionally corroded and replaced by the sparite cement. Filling the pore spaces by drusy sparite is a very important porosity-reducing factor. Sometimes the invasion process took place by Mg-bearing solution causing pore filling with micro-dolosparite and xenotopic dolosparite mosaics, e.g., dolomitic quartz arenite microfacies of Alif member (Al-Azazi 2010).

Porosity and permeability, in general, decrease by increasing depth which may be attributed to increasing cementation and compaction with depth.

For the Alif and Seen members, kaolinite is the most important clay mineral, found as booklets filling the pore spaces and causing reducing of pore spaces. Iron oxides cement may reach up to 30 % in the ferruginous quartz arenite sandstones of the studied samples (Al-Azazi 2010).

Nabawy (2013) stated that filling pore spaces by dolomitization process reduces the pore volume, while selective dolomitization causes pore volume increasing. At advanced stages of dolomitization including pervasive dolomitization and aggrading neomorphism, the pore network is thought to be

completely obliterated. Dolomitization process in Alif member is mostly selective to mid-stage, pervasive without aggrading neomorphism, increasing the pore network, and sometimes filling pores.

Petrophysical interrelationships

Alif 003 well

Based on the petrophysical behavior, the obtained data for samples from Alif 003 well were classified into three petrophysical facies. The bulk density σ_b values are the net result of both the grain and pore phase, of the grain density σ_g and porosity \varnothing_{He} . The bulk density is mostly dependant on porosity with highly reliable interrelationships ($r \geq -0.987$, Fig. 4a), but no relationship can be established with the grain

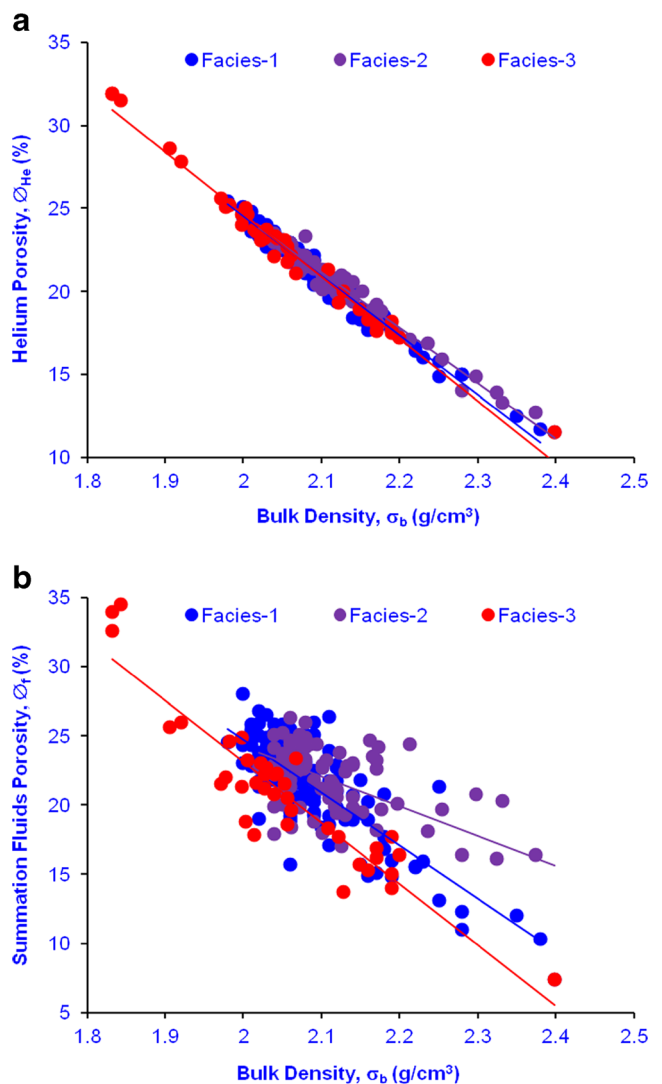


Fig 4 Plotting the bulk density versus: **a** helium porosity \varnothing_{He} , and **b** summation fluid porosity \varnothing_f for Alif member, Alif 003 well

density ($r \leq -0.55$). This may be due to the consistency of the grain density data which are in between 2.62 and 2.72 g/cm³. The bulk density–helium porosity relationship seems to be more reliable than that with the summation fluids porosity \varnothing_f which shows relatively more dispersion ($r \leq -0.92$, Fig. 4b) than the \varnothing_{He} . Bulk density of the present samples can be calculated in terms of porosity data using the following equations.

Facies-1.

$$\varnothing_{He} = 91.3 - 33.42\sigma_b \quad (r = -0.98)$$

$$\varnothing_f = 101.3 - 38.3\sigma_b \quad (r = -0.80)$$

Facies-2.

$$\varnothing_{He} = 91.3 - 33.42\sigma_b \quad (r = -0.98)$$

$$\varnothing_f = 67.1 - 21.5\sigma_b \quad (r = -0.59)$$

Facies-3.

$$\varnothing_{He} = 99.7 - 37.5\sigma_b \quad (r = -0.99)$$

$$\varnothing_f = 111.5 - 44.2\sigma_b \quad (r = -0.93)$$

The statistical constants and multiplication factors of the $\varnothing_{He}-\sigma_b$ are similar and too close to each other, so they can be extrapolated into one general equation for the Alif 003 samples as follows.

$$\varnothing_{He} = 95.6 - 35.5\sigma_b \quad (r = -0.987)$$

Dispersion of the summation fluids porosity data is ensured by plotting it against the \varnothing_{He} as in Fig. 5, where data are not best fitted. This dispersion may be raised up during coring process,

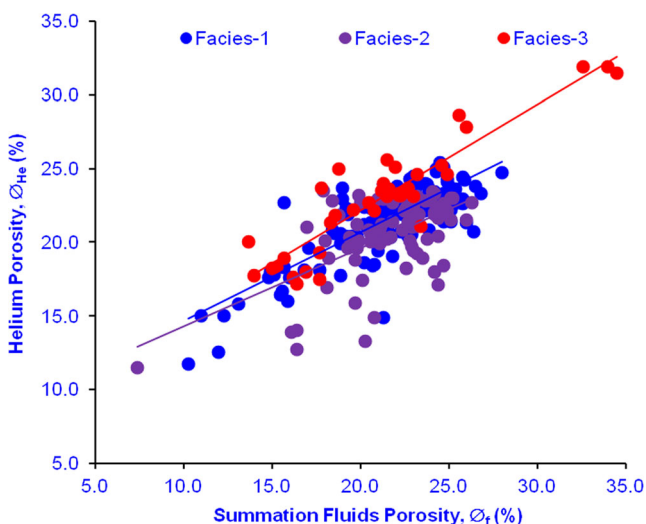


Fig 5 Plotting the helium porosity \varnothing_{He} versus the summation fluids porosity \varnothing_f for Alif 003 samples, Sab'atayn basin, Yemen

tubing, transfer, and handling of the core samples. However, to achieve more precision, missed and anomalous \varnothing_f can be calculated in terms of \varnothing_{He} using the following set of equations.

Facies-1.

$$\varnothing_{He} = 8.63 - 0.60\varnothing_f \quad (r = 0.79)$$

Facies-2.

$$\varnothing_{He} = 8.99 - 0.53\varnothing_f \quad (r = 0.57)$$

Facies-3.

$$\varnothing_{He} = 7.72 - 0.72\varnothing_f \quad (r = 0.92)$$

Horizontal permeability (K) for the studied samples are mostly ranked as very good to excellent values reaching up to 13,500 md. Permeability values for Alif 003 samples were plotted against the helium \varnothing_{He} and summation fluids porosity \varnothing_f (Fig. 6a and b, respectively). It is mostly dependant on porosity with more reliable relationship with \varnothing_{He} rather \varnothing_f . Facies-2 shows some dispersion of the $K-\varnothing_f$ data ($r=0.57$) which may be attributed to the dispersion of \varnothing_f data as shown in Figs. 5 and 6.

The calculated regression equations for these relations have the forms:

Facies-1.

$$K = 9 \times 10^{-9} \varnothing_{He}^{8.61} \quad (r = 0.92)$$

$$K = 7 \times 10^{-5} \varnothing_f^{5.70} \quad (r = 0.82)$$

Facies-2.

$$K = 2.5 \times 10^{-3} \varnothing_{He}^{4.83} \quad (r = 0.86)$$

$$K = 1.49 \times \varnothing_f^{2.65} \quad (r = 0.57)$$

Facies-3.

$$K = 3.0 \times 10^{-10} \varnothing_{He}^{9.09} \quad (r = 0.93)$$

$$K = 2 \times 10^{-6} \varnothing_f^{6.51} \quad (r = 0.82)$$

So, calculating permeability in terms of helium porosity is more precise than that in terms of summation fluids porosity.

Alif 005 well

Samples from Alif 005 well are representative for Alif and Seen members with much less thickness and less potential petrophysical parameters. Based on the petrophysical behavior, Alif and Seen members were classified into four facies.

The same porosity, permeability, and density relationships are established for samples from Alif 005 well in the SW of

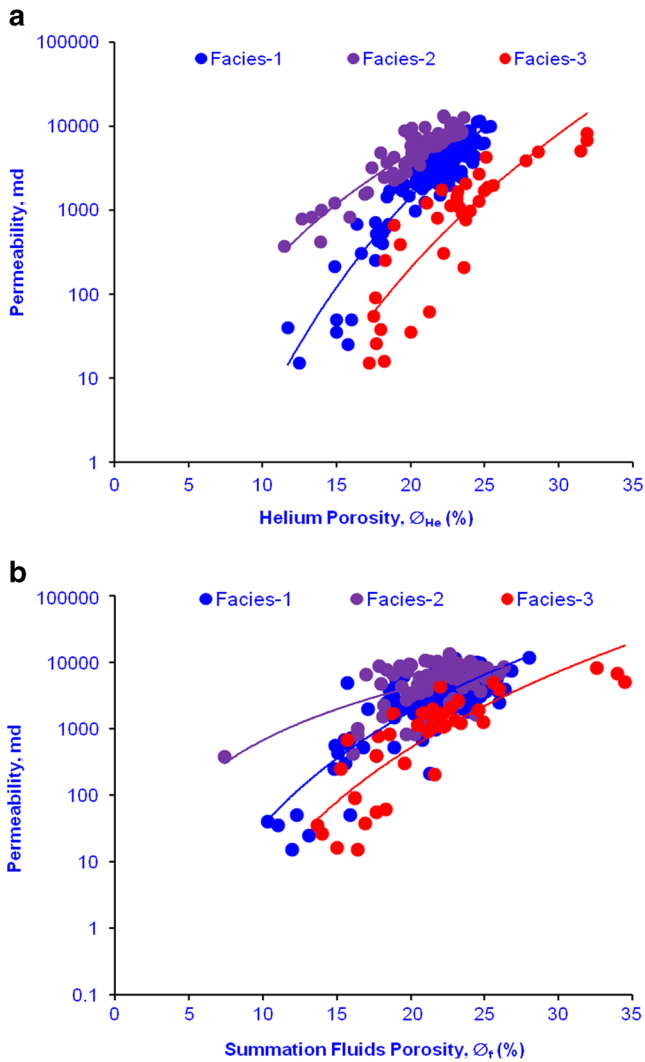


Fig 6 Plotting permeability versus: **a** helium porosity ϕ_{He} , and **b** summation fluids porosity ϕ_f for Alif 003 samples, Sab'atayn basin, Yemen

block-18, but in general with more dispersion and less reliability. The bulk density is mostly attributed to the pore volume in direct proportional relationship (Fig. 7). The relationships with ϕ_{He} are more reliable ($-0.98 \leq r$) than that with ϕ_f ($r \leq -0.76$). The relatively dispersed data ϕ_f for the facies-4 caused unreliable relationship. Porosity can be calculated in terms of bulk density of Alif and Seen members using the following equations.

Facies-1, Alif member.

$$\phi_{He} = 98.2 - 36.94\sigma_b \quad (r = -0.994)$$

$$\phi_f = 89.8 - 33.1\sigma_b \quad (r = -0.76)$$

Facies-2, Alif member.

$$\phi_{He} = 91.7 - 33.89\sigma_b \quad (r = -0.982)$$

$$\phi_f = 105.1 - 39.4\sigma_b \quad (r = -0.67)$$

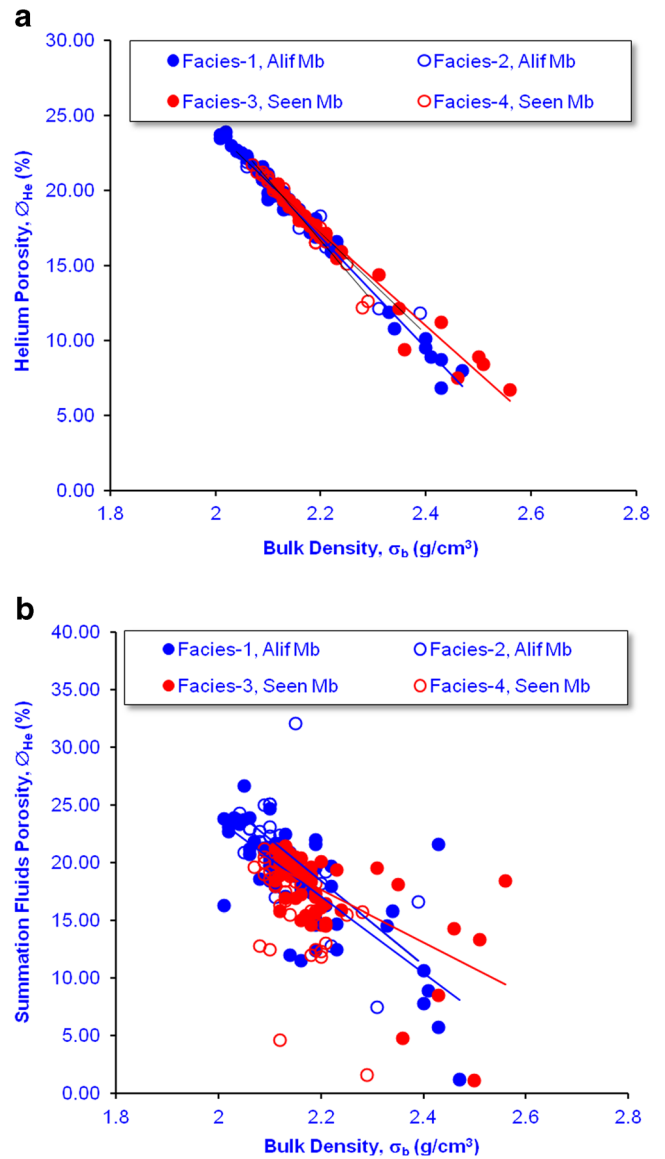


Fig 7 Plotting the bulk density versus: **a** helium porosity ϕ_{He} , and **b** summation fluids porosity ϕ_f for Alif and Seen members in Alif 005 well, Sab'atayn basin, Yemen

Facies-3, Seen member.

$$\phi_{He} = 86.1 - 31.3\sigma_b \quad (r = -0.986)$$

$$\phi_f = 67.6 - 22.7\sigma_b \quad (r = -0.64)$$

Facies-4, Seen member.

$$\phi_{He} = 107.1 - 41.1\sigma_b \quad (r = -0.987)$$

The slope and the intercept of the former equations have more or less too close values; so as the case of Alif 003 samples, they can be processed as one facies expressed by a general equation for the Alif 005 samples as follows.

$$\phi_{He} = 92.2 - 34.1\sigma_b \quad (r = -0.977)$$

Due to the inconsistency of grain density values of Facies-3, maybe due to slight variation of the mineralogical composition, the bulk density of Facies-3 increases with increasing grain density for Facies-3 (Fig. 8).

Facies-3, Seen member.

$$\sigma_g = 0.19\sigma_b + 2.25 \quad (r = 0.76)$$

Similar to the obtained \varnothing_{He} - \varnothing_f relationships of Alif 003 samples, relationships have been obtained for Alif 005 samples but with less correlation coefficient as follows. As mentioned above, due to the dispersion of for \varnothing_f of Facies-4, no relationship was established (Fig. 9).

Facies-1, Alif member.

$$\varnothing_{He} = 0.62\varnothing_f + 6.94 \quad (r = 0.73)$$

Facies-2, Alif member.

$$\varnothing_{He} = 0.44\varnothing_f + 9.88 \quad (r = 0.73)$$

Facies-3, Seen member.

$$\varnothing_{He} = 0.59\varnothing_f + 6.92 \quad (r = 0.65)$$

The horizontal permeability ‘K’ for the studied Alif and Seen members show great variation between 0.23 up to 3,824 md and ranked as impermeable to excellent permeability (Nabawy et al. 2009). Permeability of Alif and Seen samples was plotted versus summation fluids and helium porosity (Fig. 10). Permeability is dependent mostly on the helium porosity with much more reliable relationships ($0.71 \leq r \leq 0.94$) than that with the summation fluids porosity ($r \leq 0.64$). The dispersion of \varnothing_f caused unreliable relationships with ‘K’ for Facies-1 and Facies-4, where the correlation coefficient is less than 0.5. So, it is stated that permeability can be calculated in terms of \varnothing_{He} rather than the \varnothing_f disturbed data as follows.

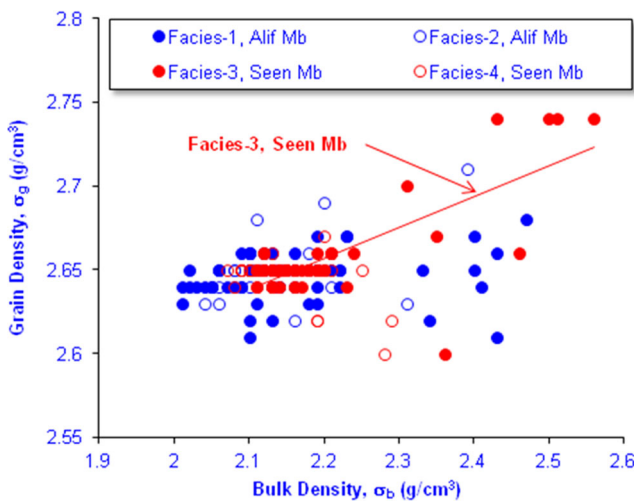


Fig 8 Plotting bulk density σ_b versus grain density of Alif and Seen members in Alif 005 well, Sab'atayn basin, Yemen

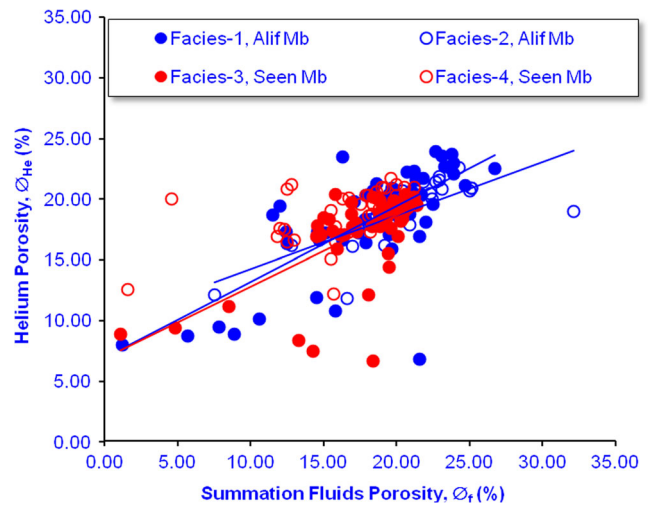


Fig 9 Plotting the helium porosity \varnothing_{He} versus the summation fluids porosity \varnothing_f for Alif 005 samples, Sab'atayn basin, Yemen

Facies-1, Alif member.

$$K = 8 \times 10^{-6} \varnothing_{He}^{5.29} \quad (r = 0.71)$$

Facies-2, Alif member.

$$K = 1.8 \times 10^{-3} \varnothing_{He}^{3.58} \quad (r = 0.77)$$

$$K = 3.03 \varnothing_f^{1.80} \quad (r = 0.64)$$

Facies-3, Seen member.

$$K = 2 \times 10^{-4} \varnothing_{He}^{1.89} \quad (r = 0.94)$$

$$K = 1.2 \varnothing_f^{1.72} \quad (r = 0.56)$$

Facies-4, Seen member.

$$K = 6 \times 10^{-11} \varnothing_{He}^{9.08} \quad (r = 0.69)$$

So, it is recommended to apply the relationships obtained between K and \varnothing_{He} , as well as the bulk density with \varnothing_{He} to precisely calculate the missed data for both Alif and Seen members in Alif field. Relationships with \varnothing_f are not recommended to be used for that target. Also, \varnothing_f is not recommended to be used for the reservoir discrimination purpose; it is only K, \varnothing_{He} , and bulk density.

Reservoir zonation

A reservoir zonation is term referring to “a statistical process applied for a given reservoir to slice and discriminate it based on its oil potentiality evaluated from its measured and calculated petrophysical data.” Based on the interpretation

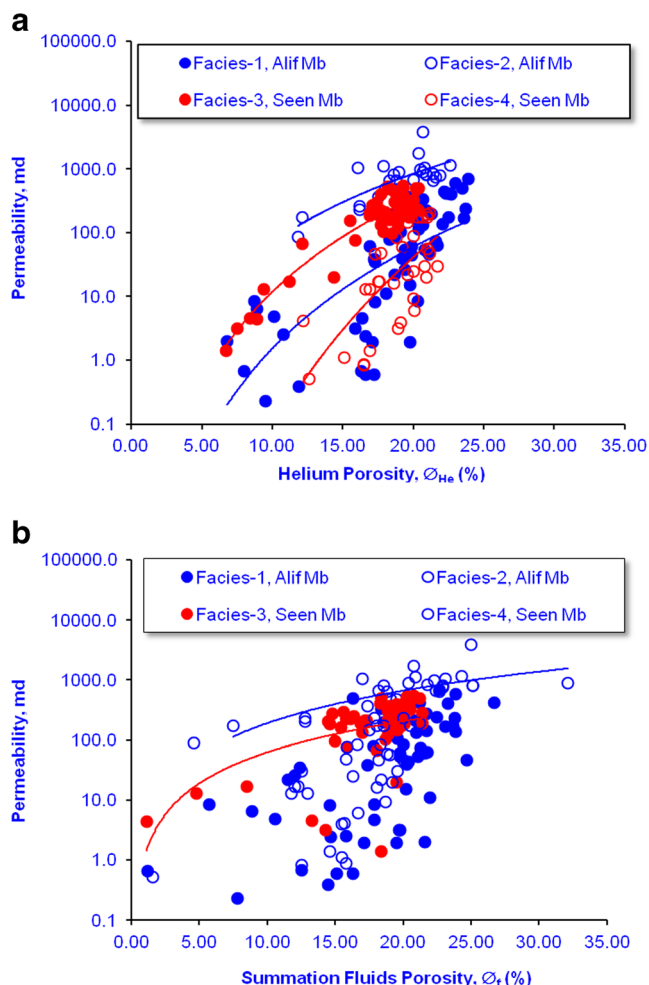


Fig 10 Plotting permeability versus: **a** helium porosity ϕ_{He} , and **b** summation fluids porosity ϕ_f for Alif and Seen members, Alif 005 well, Sab'atayn basin, Yemen

of the X–Y plots for the different measured and calculated petrophysical data, it is preferred to use the helium porosity ϕ_{He} and the horizontal permeability K_h values where both parameters show less scattering and well-trended data, as well as high reliable relationships with the other parameters. The RQI and FZI, as well as water and oil saturations ‘Sw’ and ‘So’ are very important parameters used for evaluating the reservoir potentiality and slicing the given reservoir. Some proposed ranks are given in Table 2 to help in the slicing and discrimination process.

The reservoir zonation and discrimination has been done by accumulating depths having same reservoir rank together as main flow zones and neglecting the thin streaks in between.

Alif 003 well

To perform the reservoir zonation process in both Alif 003 and Alif 005 wells, cutoff values equals to 2 are used for

porosity, permeability, RQI, FZI, and reservoir potentiality RPI (Table 2). The measured data are plotted versus depth, and the prospective reservoir zones are matched (Figs. 11 and 12).

Tracing the petrophysical data of the cored depths in Alif member in Alif 003 well to the NW of the studied area indicates good to very good RPI for the first coring depth in between 5,668.5 and 5,904.5 ft with RPI fluctuating between 4 and 5, indicating very good to excellent reservoir potentiality (Fig. 11). The rank of the RPI decrease by the end of the first core to reach 3 (good potentiality, Table 2) and continue in decreasing till reaching 1 (poor) by the end of the second coring depth (5,965.5 and 5,989.5 ft). Therefore, the total cored depth indicates good to excellent reservoir potentiality for a total depth of 222 ft, and it is fair to poor for the other 14 ft. Few streaks of low RPI are indicated by low RPI values (not less than rank 2) in the middle parts.

Therefore, it can be stated that the Alif member in Alif 003 well has a very good to excellent reservoir quality decreases downward with very good degree of homogeneity. Taking the So and Sw into consideration, the second coring show a very high Sw (65.7–95.1 %), indicating a water body. Upward through the first coring depth, except for some negligible streaks at its lower parts, So in general is more or less negligible till depth 5,832.5 ft, where the So increases slightly to less than 20 %, but Sw is still around 40 % which may indicate acceptable gas reservoir zone but not oil reservoir in the range (5,668.5–5,904.5 ft, Fig. 11).

Alif 005 well

Another reservoir zonation has been applied to the cored depths (three cored depths) in Alif 005 well taken through two members, Alif and Seen members (Fig. 12). It indicates good to very good reservoir potentiality (RPI, 3–4) in the first cored depth (5,381.5–5,405.4 ft). The second cored depth has impervious to fair reservoir quality (5,600.5–5,659.5 ft, RPI, 0–2). A total depth of 54 ft through Alif member is characterized as fair to very good reservoir; 24 ft through the first cored depth and another 30 ft in the second cored depth. The top most parts of the third cored depth still has poor reservoir potentiality index. The RPI increases to good potentiality downward in the middle parts of the third cored depth (RPI=3).

Alif and Seen members in Alif 005 well have relatively high heterogeneity in their petrophysical properties in comparison with Alif 003 well with more streaks in between causing much more vertical anisotropism, as well as pressure and permeability barriers. These barriers act as a reducing agent for the water coning chances in the reservoir body, of water drive mechanism, under excess hydrocarbon withdrawal. These barriers may be attributed

Table 2 Proposed ranks for the measured porosity and permeability data, for the RQI and FZI and for the Reservoir Potentiality Index (RPI) used to characterize and discriminate the present reservoir

Porosity (%)	Rank	Permeability (md)	Rank	RQI (μm)	Rank	FZI (μm)	Rank	RPI	Rank
0 < Ø ≤ 5	0	0 < K ≤ 1	0	0.00 < RQI ≤ 0.25	0	0.00 < FZI ≤ 1.00	0	Impervious	0
5 < Ø ≤ 10	1	1 < K ≤ 10	1	0.25 < RQI ≤ 0.50	1	1.00 < FZI ≤ 2.50	1	Poor	1
10 < Ø ≤ 15	2	10 < K ≤ 100	2	0.50 < RQI ≤ 1.00	2	2.50 < FZI ≤ 5.00	2	Fair	2
15 < Ø ≤ 20	3	100 < K ≤ 1,000	3	1.00 < RQI ≤ 2.00	3	5.00 < FZI ≤ 10.0	3	Good	3
20 < Ø ≤ 25	4	1,000 < K ≤ 10,000	4	2.00 < RQI ≤ 5.00	4	10.0 < FZI ≤ 15.0	4	Very good	4
25 < Ø	5	10,000 < K	5	5.00 < RQI	5	15.0 < FZI	5	Excellent	5

to presence of more shaley intercalations in the lower parts of both Alif and Seen member.

Taken into consideration the So and Sw readings, a reservoir zonation indicates good to very good reservoir in the first cored depth and fair in the middle parts of the second coring depth, while the water saturation increases

greatly at more depths. This zone of Alif member may be accepted as a gas reservoir with So not more than 5 %. Increasing the So up to 13 % in the upper parts of Seen member indicates another reservoir completely separated from that of Alif member. In Seen member, the Sw increases greatly after depth 5,815.5 ft changing into a thick water

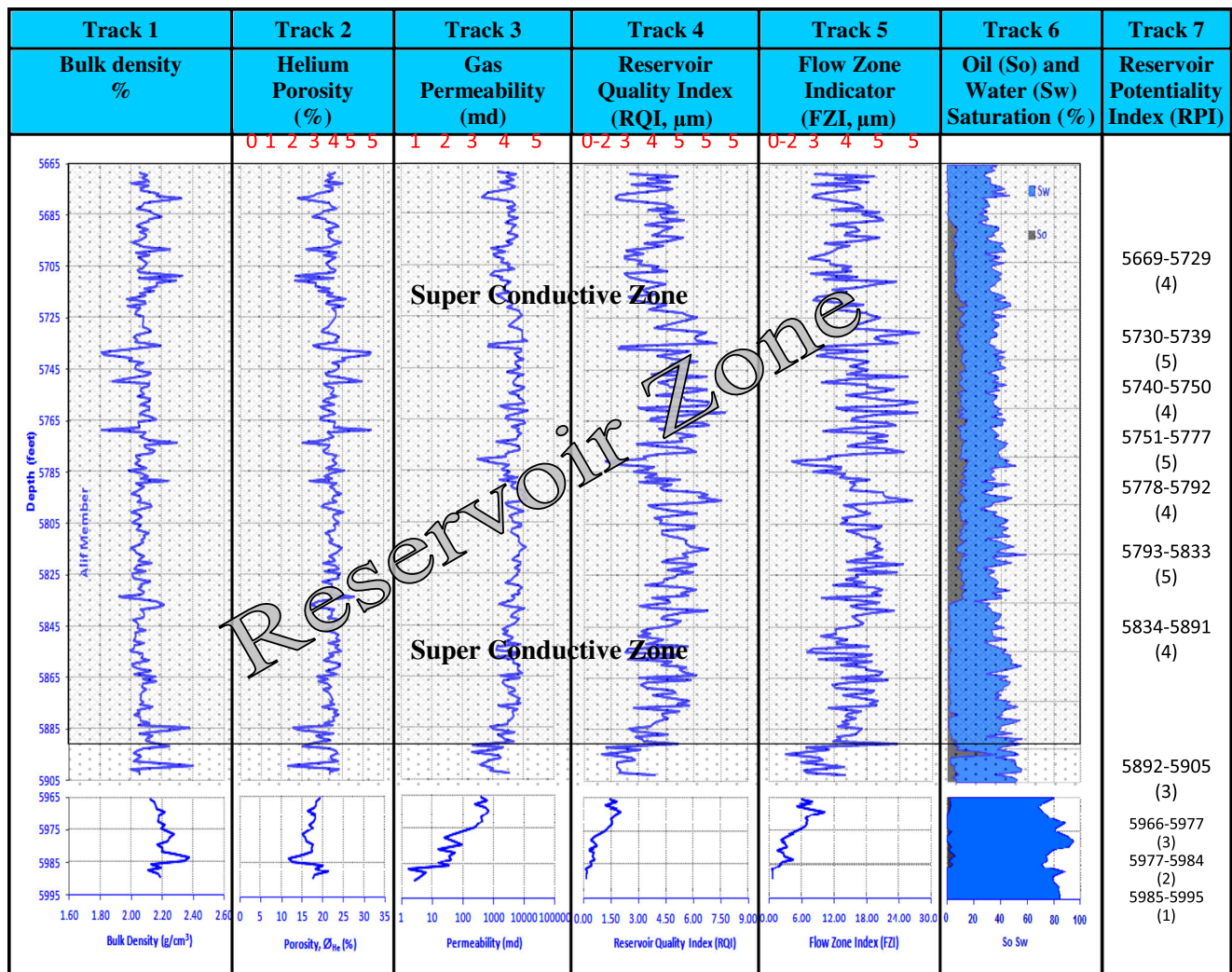


Fig 11 Vertical matching of bulk density, porosity, permeability, RQI, FZI, and reservoir potentiality (RPI) versus depth for the Alif member, Sab'atayn Formation, Alif 003 well, Sab'atayn basin, Yemen. Ranks are shown in red color

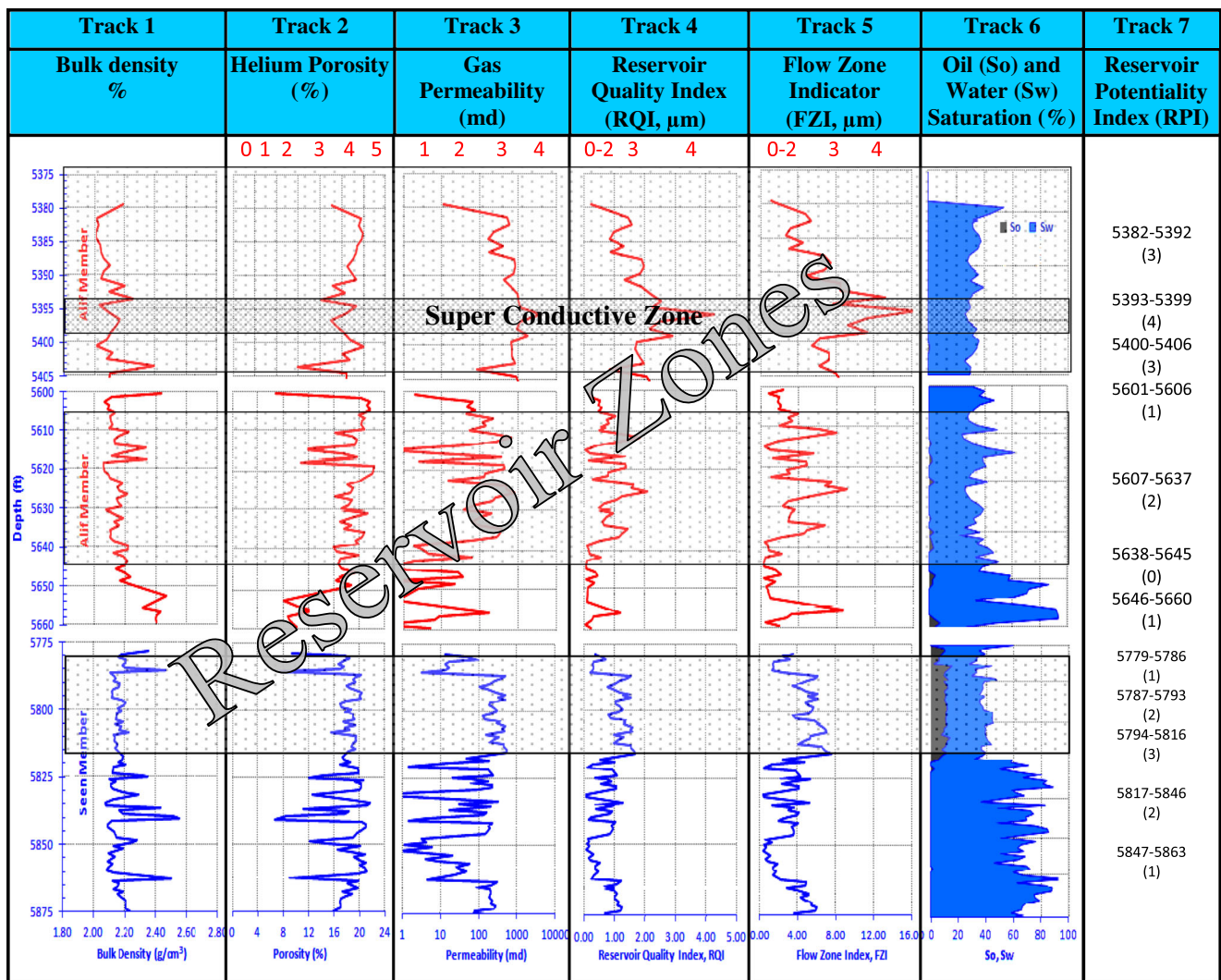


Fig 12 Vertical matching of storage capacity parameters, RQI, FZI, and reservoir potentiality RPI against depth for the Alif and Seen members, Sab'atayn Formation, Alif 005 well, Sab'atayn basin, Yemen. Ranks are shown in red color

body. Integrating the mentioned data for Alif member indicates a water drive gas reservoir (5,381.5–5,644.5 ft) while, for Seen member, poor to good gas reservoir potentiality was indicated in the top-most parts which is thought to be controlled by a water drive mechanism.

Super conductive reservoir discrimination

The concept of the RQI and the FZI of Amaefule et al. (1993) as well as RPI were used for identification and discrimination of the super conductive zones. The RQI and FZI values for the different samples are shown in Table 1, whereas the RPI is taken as the arithmetic mean of both values. Values of the mentioned parameters are, in general, higher for Alif 003 samples than Alif 005 samples. Also, they are much higher

for Alif member than Seen member. The standard deviations for the calculated RQI and FZI are relatively higher for Alif 005 samples, indicating more heterogeneity which increases to the southwest of the studied field. As shown in Figs. 11 and 12, the reservoir zonation is carried out based on cutoff value equals to 2 for the RQI, FZI, and the RPI and taken into consideration the So and Sw.

On the other hand, discriminating the super conductive zone was done using cutoff values equal to rank 4 (Table 2), indicating very good to excellent reservoir zones (Figs. 11 and 12). Based on the proposed values, the super conductive zones are estimated as 222 ft out of the total reservoir zone estimated as 236 ft for Alif 003 well (Fig. 11). The mentioned super conductive zone has very high permeability varies from 427 md up to 13,500 md and porosity from 14.9 to 31.9 %; therefore, the RQI varies from 0.93 to 7.74 μm.

The estimated super conductive zone is much thinner in the SW in Alif 005 well with more petrophysical heterogeneity and less reservoir potentiality. The super conductive zone is estimated to the SW as 6 ft out of total reservoir zones estimated as 54 ft for Alif member. This very thin horizon has permeability varies between 895 and 3,824 md, whereas porosity varies from 16.10 to 22.60 %. Taken into consideration the cutoff values that proposed for super conductive zones, Seen member has no super conductive zones (Fig. 12).

Comparing the RQI, FZI, and RPI parameters for the super conductive zones in both wells indicates higher reservoir quality for the super quality zones in Alif 003 well than that for Alif 005 well.

Alif 003 well

To define the main attributors to the RQI and the FZI parameters, both are plotted versus the measured density, porosity, and permeability (Figs. 13–16). The RQI of Alif 003 samples are dependent mostly on permeability of the different petrophysical facies ($r \geq 0.996$, Fig. 13c). It is also dependent on the bulk density (Fig. 13a) and pore volume (Fig. 13b). A set of empirical equations were derived to calculate the RQI in terms of the different petrophysical parameters of Alif 003 samples.

Facies-1, Alif member.

$$RQI = 2.5 \times 10^5 \sigma_b^{-15.3} \quad (r = -0.89)$$

$$RQI = 3.0 \times 10^{-5} \phi_{He}^{3.81} \quad (r = 0.90)$$

$$RQI = 0.10 K^{0.45} \quad (r = 0.999)$$

Facies-2, Alif member.

$$RQI = 1.8 \times 10^3 \sigma_b^{-7.89} \quad (r = -0.90)$$

$$RQI = 1.6 \times 10^{-2} \phi_{He}^{1.91} \quad (r = 0.90)$$

$$RQI = 0.15 K^{0.41} \quad (r = 0.996)$$

Facies-3, Alif member.

$$RQI = 3.5 \times 10^4 \sigma_b^{-14.0} \quad (r = -0.84)$$

$$RQI = 5.0 \times 10^{-6} \phi_{He}^{4.05} \quad (r = 0.83)$$

$$RQI = 0.09 K^{0.46} \quad (r = 0.997)$$

The high reliability of the obtained equations is due to the homogeneity of the petrophysical behavior of the studied samples. For Facies-3, the bulk density and pore

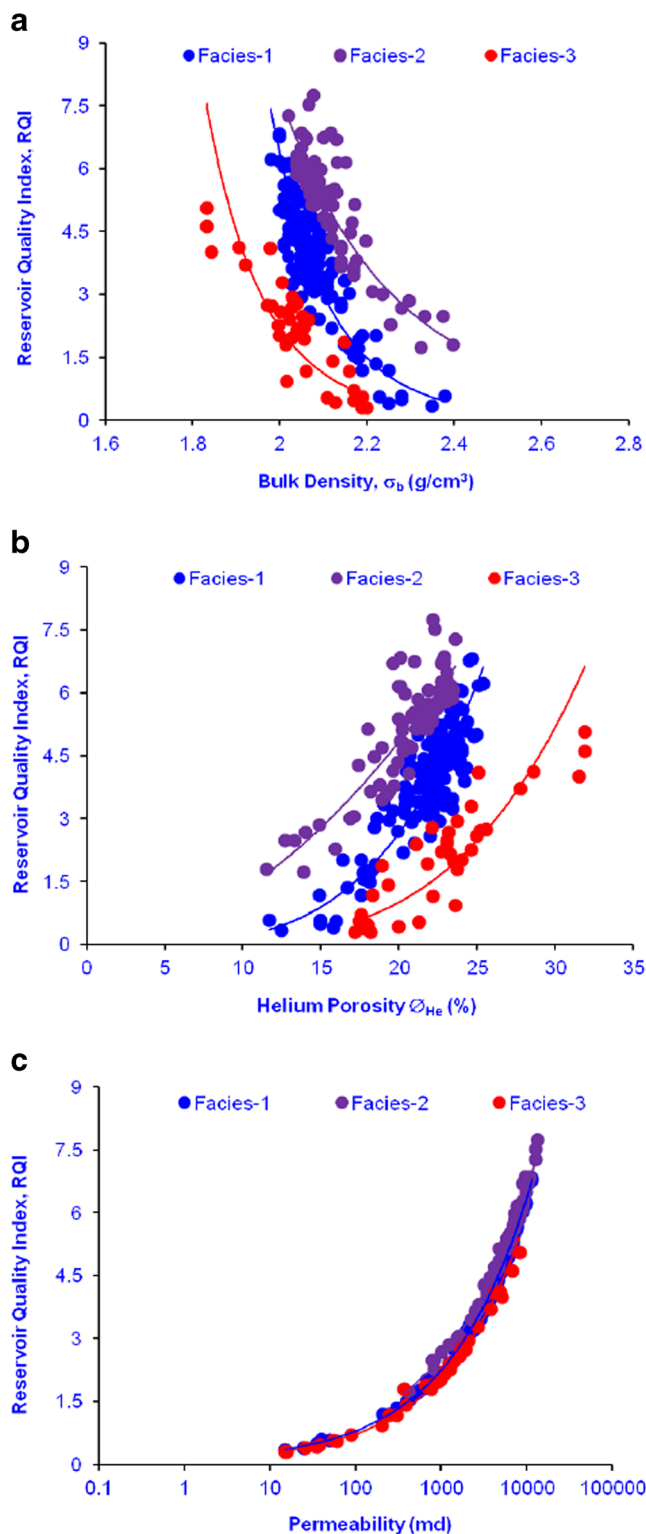


Fig 13 Plotting the RQI versus: a bulk density σ_b , b helium porosity ϕ_{He} , and c horizontal permeability 'K' for Alif samples from Alif 003 well, Sab'atayn Formation, Yemen

volume are less homogeneous than the permeability values. Therefore, it is recommended to calculate the RQI in terms of permeability.

Plotting the FZI values of the same well versus the same parameters (Fig. 14) shows that the FZI can be calculated in terms of these parameters using a set of exponential equations as follows.

Facies-1, Alif member.

$$FZI = 2.4 \times 10^4 \sigma_b^{-10.3} \quad (r = -0.81)$$

$$FZI = 0.005 \varnothing_{He}^{2.57} \quad (r = 0.82)$$

$$FZI = 0.95 K^{0.33} \quad (r = 0.98)$$

Facies-2, Alif member.

$$FZI = 1.7 \times 10^2 \sigma_b^{-2.95} \quad (r = -0.62)$$

$$FZI = 2.4 \varnothing_{He}^{0.69} \quad (r = 0.60)$$

$$FZI = 3.85 K^{0.19} \quad (r = 0.85)$$

Facies-3, Alif member.

$$FZI = 5.0 \times 10^{-3} \sigma_b^{-9.5} \quad (r = -0.72)$$

$$FZI = 0.001 \varnothing_{He}^{2.74} \quad (r = 0.71)$$

$$FZI = 0.58 K^{0.35} \quad (r = 0.97)$$

The reliability of the obtained equations for FZI is less than that with the RQI, which may be attributed to the pore volume distribution.

For the Alif 003 samples, permeability is the main contributor to the RQI ($r \geq 0.996$) and FZI ($r \geq 0.85$), i.e., it is the main controlling factor for the reservoir potentiality.

Alif 005 well

Similar to the statistical processing of samples of well Alif 003, the RQI and FZI values of Alif and Seen samples, Alif 005 well, were plotted versus the bulk density, helium porosity, and permeability (Figs. 15 and 16). The permeability stills the main contributor to the RQI with very high reliability.

From the statistical processing of the valid petrophysical data in the present study, a number of empirical equations are introduced to be used for calculating both the RQI and FZI values in terms of the valid bulk density, helium porosity, and horizontal permeability.

Facies-1, Alif member.

$$RQI = 1.7 \times 10^4 \sigma_b^{-13.8} \quad (r = -0.71)$$

$$RQI = 9.0 \times 10^{-4} \varnothing_{He}^{2.14} \quad (r = 0.63)$$

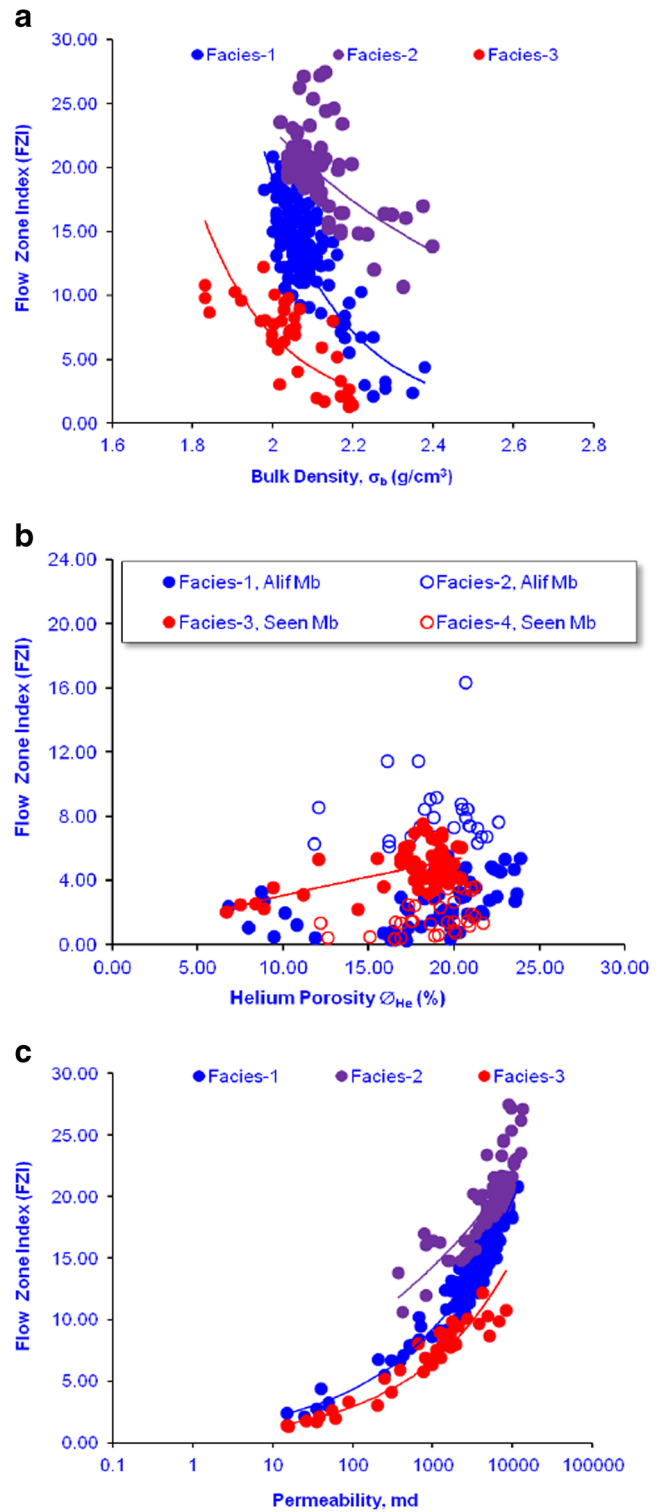


Fig 14 Plotting the FZI versus: **a** bulk density σ_b , **b** helium porosity \varnothing_{He} , and **c** horizontal permeability ‘K’ for Alif samples from Alif 003 well, Sab’atayn Formation, Yemen

$$RQI = 0.09 K^{0.45} \quad (r = 0.994)$$

$$FZI = 0.59 K^{0.34} \quad (r = 0.91)$$

Fig 15 Plotting the RQI versus; **a** bulk density σ_b , **b** helium porosity \varnothing_{He} , and **c** horizontal permeability ‘K’ for Alif and Seen samples from Alif 005 well, Sab’atayn Formation, Yemen

Facies-2, Alif member.

$$RQI = 2.3 \times 10^2 \sigma_b^{-6.35} \quad (r = -0.76)$$

$$RQI = 4.2 \times 10^{-2} \varnothing_{He}^{1.29} \quad (r = 0.69)$$

$$RQI = 0.14 K^{0.40} \quad (r = 0.981)$$

$$FZI = 2.26 K^{0.19} \quad (r = 0.66)$$

Facies-3, Seen member.

$$RQI = 4.4 \times 10^3 \sigma_b^{-10.7} \quad (r = -0.90)$$

$$RQI = 3.9 \times 10^{-3} \varnothing_{He}^{1.95} \quad (r = 0.91)$$

$$RQI = 0.12 K^{0.41} \quad (r = 0.997)$$

$$FZI = 1.5 \times 10^2 \sigma_b^{-4.47} \quad (r = -0.67)$$

$$FZI = 0.49 \varnothing_{He}^{0.79} \quad (r = 0.66)$$

$$FZI = 1.67 K^{0.20} \quad (r = 0.88)$$

Facies-4, Seen member.

$$RQI = 6.0 \times 10^6 \sigma_b^{-21.9} \quad (r = -0.66)$$

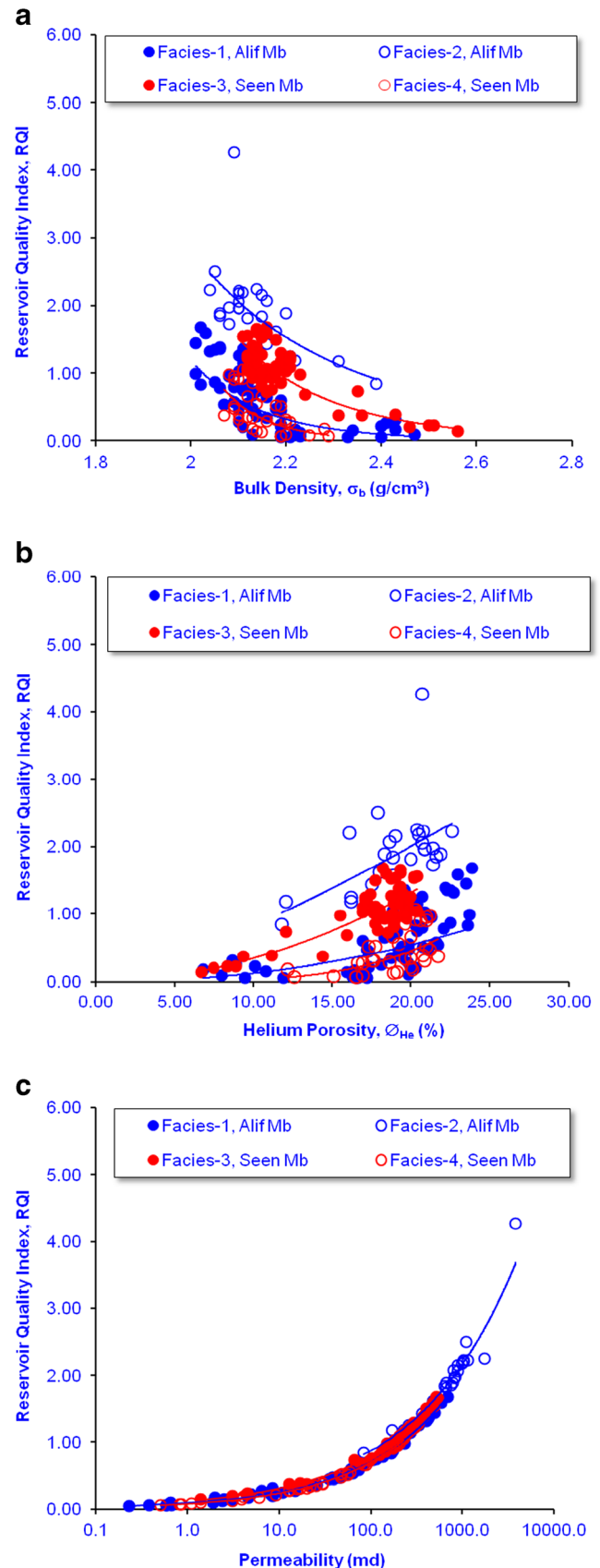
$$RQI = 2.0 \times 10^{-6} \varnothing_{He}^{4.04} \quad (r = 0.65)$$

$$RQI = 0.08 K^{0.47} \quad (r = 0.998)$$

$$FZI = 0.42 K^{0.41} \quad (r = 0.97)$$

From the statistical processing of the whole data, it is recommended to use the valid permeability data to extrapolate the RQI and FZI values for the other wells in the Alif field. It can be extrapolated for further activities at the borders of the field.

On plotting the FZI versus the bulk density and porosity, scattered distribution data with unreliable relationships ($r < 0.5$) were obtained. Consequently, using the porosity and bulk density values for calculating the quality control parameters is not recommended for use in calculating the flow zone index using the present equations and to use the quality



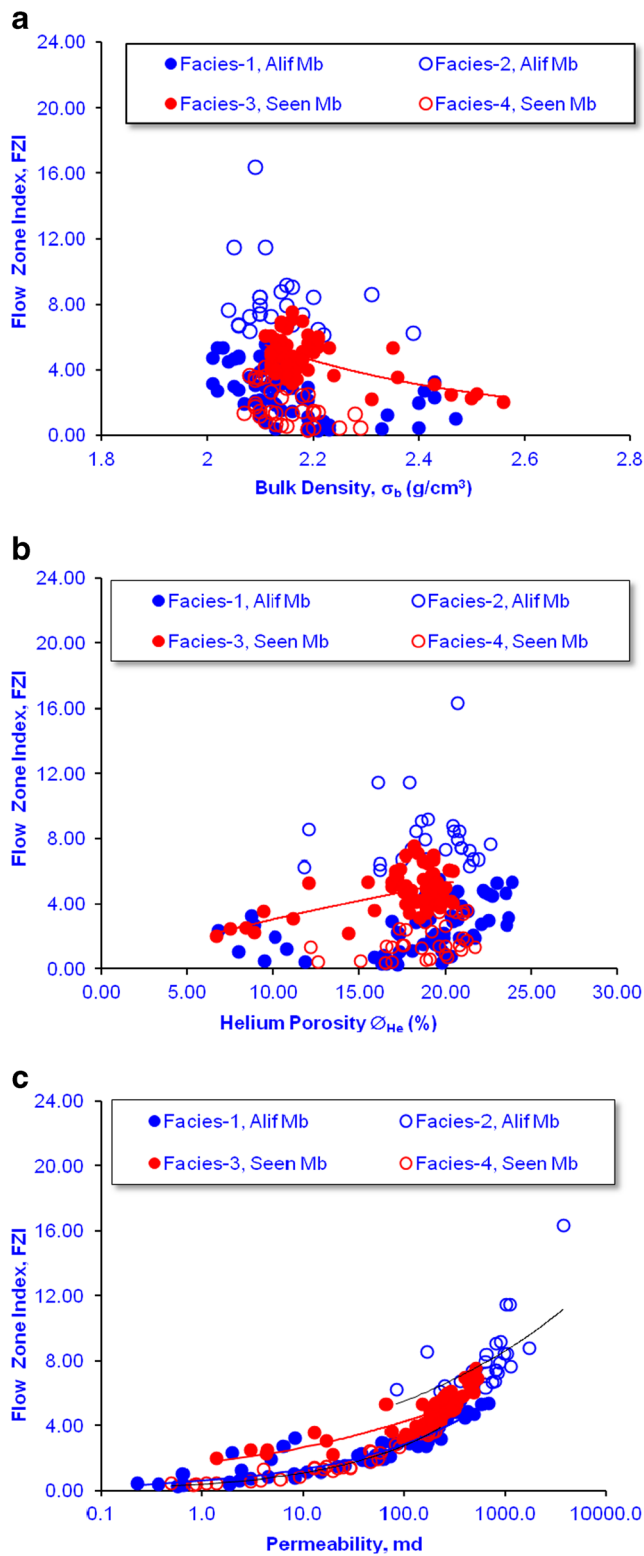


Fig 16 Plotting of the FZI versus **a** bulk density σ_b , **b** helium porosity ϕ_{He} , and **c** horizontal permeability ‘ K ’ for Alif and Seen samples, Alif 005 well, Sab’atayn Formation, Yemen

control parameters for each well to predict the missed density and porosity data within the same well.

The statistical values of the RQI- K for both Alif 003 and Alif 005 wells are too close to each other, where the multiplication factor varies between 0.08 and 0.15, whereas the exponent varies from 0.40 to 0.47 with very high reliability ($0.981 \leq r \leq 0.999$). On the other side, the exponent values of the FZI- K are too close to each other, where the exponent varies from 0.19 to 0.41 with very high reliability ($0.66 \leq r \leq 0.91$). So, the following can be applied to calculate the RQI and the FZI of the different facies of Alif and Seen members in Alif field in terms of ‘ K ’ as follows.

$$RQI = 0.09 K^{0.47} \quad (r = 0.998)$$

$$FZI = 0.63 K^{0.38} \quad (r = 0.938)$$

Conclusions

The helium porosity values for the studied sandstones of Alif and Seen members of the Sab’atayn Formation in Alif field show a main contribution to both of the bulk density values and the horizontal permeability ‘ K ’ with high reliable proportional relationships. A set of equations was introduced relating the studied petrophysical parameters to each other. Both permeability and bulk density can be precisely calculated in terms of porosity using the present empirical equations.

Matching the studied data vertically against depth enabled reservoir zonation and discrimination into high potential and poor zones.

Using the RQI, the FZI and the RPI enabled discrimination of a main reservoir body of 247 ft thickness (ranked as very good to excellent reservoir (RPI, 4–5), Alif member, Alif 003 well to the northeast of the studied area.

The mentioned reservoir is ranked as very good to excellent reservoir with RPI 4–5. To the southwest of Alif field, two thin and relatively low potential bodies can be detected of thickness 24 and 30 ft. They have good to very good reservoir potentiality (RPI, 3–4). Downward through Seen member, another reservoir body of thickness 29 ft can be detected of fair to good potentiality (RPI, 3–4).

Taken into consideration water and oil saturations, the detected reservoirs are mostly gas reservoirs of composed drive mechanism (water and gas cap drive).

It is recommended to use the concept of RPI to discriminate the main super conductive zones in a given reservoir. Summation fluid porosity is not recommended to be used for calculating the RQI and FZI parameters, while the permeability is highly recommended to be used for this target.

Acknowledgment The authors would like to acknowledge Yemen Safer Exploration and production operation Company (SEPOC) for release the core analyses reports and the license for data processing and interpretation.

We would like also to thank the reviewers for their comments that greatly improved and reconstructed the manuscript. Thanks are also due to the editor Prof. El-Amri whose patience and insightful suggestion has lead to a new concise revised version.

References

- Abou Khadrah A (1982) A review of the sedimentological evolution of Yemen Arab Republic. *Bull Fac Sci San'a Univ* 2:39–55
- Abou Khadrah A, El-Anbaawy M, El-Fawal F (1983) Stratigraphy of the Tawilah Sandstone in the environ of Sana'a, Yemen Arab Republic. *Bull. Fac. Sci. Zagazig Univ* 5:294–321
- Ahlbrandt, Th.S., 2002. Madbi Amran/Qishn total petroleum system of the Ma'rib-Al Jawf/Shabwah, and Masila-Jeza basins, Yemen. Published in the Central Region, Denver, Colorado, U.S. Geological Survey, version 1, 33 p.
- Al-Azazi, N.A.S., 2010. Subsurface geological studies and hydrocarbon potentialities of the Sab'atayn Formation (Upper Jurassic) in Alif oil field, Marib-Shabwa basin, Republic of Yemen. Unpublished M.Sc. Thesis, Menoufiya Univ., Egypt, 236p.
- Al-Dhafeeri AM, Nasr-El-Din HA (2007) Characteristics of high-permeability zones using core analysis, and production logging data. *J Petrol Sci and Eng* 55:18–36
- Al-Thour K (1997) Facies sequences of Middle–Upper Jurassic carbonate platform (Amran Group) in the Sana'a region Republic of Yemen. *Marine and petrol Geol* 14(6):643–660
- Al-Thour, K., 2000. Diagenesis of the Middle–Upper Jurassic carbonate platform (Amran Group), Yemen: In Middle East models of Jurassic/Cretaceous carbonate systems, A. Al-Sharhan and R. Scott (eds.), SEPM Special publication, no. 69, USA, 155–172
- Al-Wosabi MA (2003) Three new foraminiferal species from the Amran group. *Yemen Republic Egypt J Paleontol* 3:87–90
- Al-Wosabi MA (2005) Stratigraphy of the Middle–Late Jurassic foraminifera in the western and northwestern regions of Sana'a Basin. *Repub of Yemen Fac Sci Bull Sana'a Univ* 18:71–114
- Alaug, A.S., Al-Wosabi, K.A. & Al-Ramsy, J., 2008. Evaluation of Late Jurassic source rocks, Al-Jawf Basin, NE central Yemen. *Bull. Tethys Geological Soc., Cairo*, 3, 99–110.
- Alaug AS, Leythaeuser D, Bruns B, Ahmed AF (2011) Source rock evaluation, modelling, maturation, and reservoir characterization of the block 18 oilfields, Sab'atayn Basin. *Yemen Iran J Earth Sci* 3:134–152
- Amaefule, J.O., Altunbay, M., Tiab, D., Kersey, D.G. & Keelan, D.K., 1993. Enhanced reservoir description: using core and log data to identify hydraulic (flow) units and predict permeability in uncored intervals/wells. SPE 26436. Presented at the Annual Technical Conference and Exhibition, Houston, TX, 3–6.
- As-Saruri MA, Sorkhabi R, Baraba R (2010) Sedimentary basins of Yemen: their tectonic development and lithostratigraphic cover. *Arab J GeoSci* 3:515–527
- Beydoun ZR (1964) The stratigraphy and structure of the eastern Aden Protectorate. *Overseas Geology and Mineral Resources, Suppl. Ser., Bull. Suppl.*, 5. HMSO, London
- Beydoun ZR, Greenwood JEGW (1968) Aden Protectoate and Dhufar, in *Lexique Stratigraphique International*, vol III., *Asie* (L. Dubertret, ed.). CNRS, Paris, Fasc, 1062 p
- Beydoun ZR (1991) Arabian plate hydrocarbon geology and potential—a plate tectonic approach, *American Association Petroleum Geologists. Studies in Geology* 33:77
- Beydoun ZR, Bamahmoud MO, Nani ASO (1993) The Qishn Formation, Yemen: lithofacies and hydrocarbon habitat. *Marine and Petrol Geol* 10:364–372
- Beydoun ZR, As-Saruri M, Baraba RS (1996) Sedimentary basins of the Republic of Yemen: their structural evolution and geological characteristics. *Revue Institut Francais Petrole* 51:763–775
- Beydoun ZR (1997) Introduction to the revised Mesozoic stratigraphy and nomenclature for Yemen. *Marine and Petrol Geol* 14:617–629
- Beydoun, Z.R., As-Saruri, M.A.L., El-Nakhal, H., Al-Ganad, I.N., Baraba, R.S., Nani, A.S.O. & Al-Aawah, M.H., 1998. *International Lexicon of Stratigraphy*, v. III, 2nd ed. International Union of Geological Sciences and International Commission on Stratigraphy, Ministry of Oil and Mineral Resources, Republic of Yemen, 34, 245.
- Bosence DW (1997) Mesozoic rift basins of Yemen. *Marine and Petrol Geol* 14:611–616
- Bott WF, Smith BA, Oakes G, Sikander AH, Ibrahim AI (1992) The tectonic framework and regional hydrocarbon prospectivity of the Gulf of Aden. *J Petrol Geol* 15:211–243
- Brannan J, Gerdes KD, Newth IR (1997) Tectono-stratigraphic development of the Qamar Basin, eastern Yemen. *Marine and Petrol Geol* 14:701–730
- Brannin J, Sahota G, Gerdes KD, Berry JAL (1999) Geological evolution of the central Marib-Shabwa basin, Yemen. *GeoArabia* 4(1):9–34
- Csato I, Habib A, Kiss K, Kocz I, Kovacs Z, Lorincz K, Milota K (2001) Play concepts of oil exploration in Yemen. *Oil and Gas J* 99(23):68–74
- Csato, I., 2005. Extensional tectonics and salt structures, Marib-Shabwa basin, Yemen. Adapted from extended abstract, AAPG Annual Convention, Dallas, April 17–21, 2004
- Diggens, J., Dixon, R., Downie, R., Harvis, J., Jakubowski, M., Lucas, P., Mathews, S., Southwood, D. & Ventris, P., 1988. A geological model for the evolution of the Marib-Jawf basin, Y.A.R. Robertson Research International Limited, Unpublished Internal report, No. 6216/lib.
- Dutton SP, Land LS (1988) Cementation and burial history of a low-permeability quartz arenite, Lower Cretaceous Travis Peak Formation, East Texas. *Geol Soc Am Bull* 100:1271–1282
- El-Anbaawy M (1984) Contribution to the lithostratigraphic subdivisions of the Amran Sequences in the Yemen Arab Republic (Y.A.R.). *Bull. Fac. Sci Sana'a Univ* 4:65–84
- El-Anbaawy M, Al-Thour KA (1989) Sedimentological evolution, diagenesis and hydrocarbon potentiality of Late Jurassic carbonates, Eastern Region, Yemen Arab Republic. *J Univ Kuwait Sci* 16(2): 401–421
- El-Nakhal H (1990) Surdud Group; a new lithostratigraphic unit of Jurassic age in Yemen Arab Republic. *J King Saud Univ Sci* 2: 125–143
- Ellis AC, Kerr HM, Cornwell CP, Williams DO (1996) A tectonostratigraphic framework for Yemen and its implications for hydrocarbon potential. *Petrol Geosci* 2:29–42
- Gendrot, C., 1995. Interpretation of electrical imaging logs (FMSFMI) within the wells of Total, Yemen, In: *Rift sedimentation and tectonics in the Red Sea-Gulf of Aden region*, ed. D. W. J. Bosence, p. 26, Abstract volume, Sana'a, Yemen.
- Geukens, F., 1966. *Geology of the Arabian Peninsula*. Translated from French by S.D. Bowers, Professional paper, 560-B, USA Geological Survey. Washington, DC, 23p
- Greenwood, W.R., Anderson, R.E., Fleck, R.J. & Roberts, R.J., 1980. Precambrian geologic history and plate tectonic evolution of the Arabian Shield. Jiddah, Saudi Arabia, Directorate General of Mineral Resources, Ministry of Petroleum and Mineral Resources, 24, 35 p
- Haitham FMS, Nani ASO (1990) The Gulf of Aden rift: hydrocarbon potential of the Arabian sector. *J Petrol Geol* 13:211–220
- Hakimi MH, Abdullah WH, Shalaby MR (2011a) Organic geochemical characteristics and depositional environments of the Jurassic shales in the Masila Basin of eastern Yemen. *GeoArabia* 16:47–64

- Hakimi MH, Abdullah WH, Shalaby MR (2011b) Organic geochemical characteristics of crude oils from the Masila Basin, eastern Yemen. *Org Geochem* 42:465–476
- Hughes GW, Clarke MW (1988) Stratigraphy and rock unit nomenclature in the oil-producing area of interior Oman. *J Petrol Geol* 11:5–60
- Hughes GW, Beydoun ZR (1992) The Red Sea-Gulf of Aden: biostratigraphy, lithostratigraphy and paleoenvironments. *J Petrol Geol* 15:135–156
- Husseini MI (1989) Tectonic and deposition model of Late Precambrian–Cambrian Arabian and adjoining plates. *AAPG Bull* 73:1117–1131
- Jungwirth J, As-Saruri M (1990) Structural evolution of the platform cover on southern Arabian Peninsula (P.D.R. Yemen). *Zeitschrift für Geologische Wissenschaft* 18:505–514
- Mitchell, G. & Kohles, K. M., 1995. Depositional sequences in the Upper Jurassic of the Marib-Jawf Basin, Republic of Yemen. In: *Rift sedimentation and tectonics in the Red Sea-Gulf of Aden region* (Ed. D. W. J. Bosence) Abstract volume, Sana'a, Yemen, 44.
- Mitchell, G. & Galbiati, L., 1995. Tectonic and stratigraphic framework of the Marib-Jawf Basin, Yemen. In: *Rift sedimentation and tectonics in the Red Sea-Gulf of Aden region* (Ed. D. W. J. Bosence) Abstract volume, Sana'a, Yemen, 43.
- Nabawy BS (2013) Impacts of dolomitization on the petrophysical properties of the Cenomanian El-Halal Formation, north Sinai, Egypt. *J Arab Geosci* 6(2):359–373
- Nabawy BS, Rochette P, Géraud Y (2009) Petrophysical and magnetic Pore Network Anisotropy of Some Cretaceous sandstone from Tushka Basin, Egypt. *GJI* 177(1):43–61
- Othman A, Nabawy BS, AbdelHafeez T, Saher M, AbdelKader R (2008) Reservoir quality discrimination of the lower part of Bahariya formation, N. Qarun Oil Field, W.D. Egypt *EGS J* 6(1):81–101
- Paul, S.K., 1990. People's Democratic Republic of Yemen: a future oil province. Geological Society, London. Special Publ., (50), 329–339.
- Powers, R.W., Ramirez, L.F., Redmond, C.D. & Elberg, E.L., 1966. Sedimentary Geology of Saudi Arabia, in *Geology of the Arabian Peninsula: United States Geological Survey Professional Paper*, 560-D
- Redfern P, Jones JA (1995) The interior basins of Yemen analysis of basin structure and stratigraphy in a regional plate tectonic context. *Basin Research* 7:337–356
- Schlumberger, 1992. Looking for Yemen's hidden treasure: Schlumberger Technical Services Dubai, Middle East Well Evaluation Rev., 12, 12–29
- Seaborne, T. R., 1995. The influence of the Sabatayn evaporates on the hydrocarbon prospectivity of the eastern Shabwa Basin, Onshore Yemen. In: *Rift sedimentation and tectonics in the Red Sea-Gulf of Aden region* (Ed. D. W. J. Bosence) Abstract volume, Sana'a, Yemen, 60.
- Seaborne TR (1996) The influence of the Sabatayn evaporates on the hydrocarbon prospectivity of the eastern Shabwa Basin, onshore Yemen. *Marine and Petrol Geol* 13:963–972
- Sharland, P.R., Archer, R., Cassey, D.M., Davies, R.B., Hall, S.H., Heward, A.P., Horbery, A.D. & Simmons, M.D., 2001. Arabian Plate Sequence Stratigraphy. 371, Gulf PetroLink, Bahrain.
- Tiab, D. & Donaldson, E.C., 1996. *Petrophysics, Theory and practice of measuring reservoir rock and fluid transport properties*. 205–220, Gulf Publ. Co., Houston, Texas
- Whitehouse MJ, Windley BF, Ba-bttat MAO, Fanning CM, Rex DC (1998) Crustal evolution and terrain correlation in the eastern Arabian Shield, Yemen; geochronological constraints. *J Geologic Soc, London* 155:281–295